HEAT TRANSFER ENHANCEMENT WITH HELICAL COIL SPRING IN TUBE FLOW

A Thesis Submitted
in Partial Fulfillment of the Requirement
for the Degree of

MASTER OF TECHNOLOGY

By

ALOK TRIPATHI

to the

DEPARTMENT OF MECHANICAL ENGINEERING

INDIAN INSTITUTE OF TECHNOLOGY, KANPUR

AUGUST, 1999

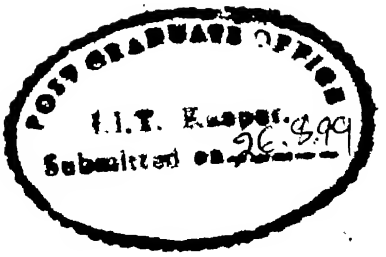

Certificate

Certified that the work contained in the thesis entitled "**HEAT TRANSFER ENHANCEMENT WITH HELICAL COIL SPRINGS IN TUBE FLOW** ", by Mr. *Alok Tripathi*, has been carried out under my supervision and that this work has not been submitted elsewhere for a degree.

Keshav Kant

(Dr. Keshav Kant)
Professor
Department of Mechanical Engineering
I.I.T.
Kanpur

August. 1999

Dedicated to
My family

Acknowledgement

I take this opportunity to express my sense of gratitude to my supervisor Prof. Keshav Kant, to whom I owe more than I can possibly express, for his warm guidance that led to the completion of this work. It was a great pleasure to work under him as a lot of care and affection was available throughout. I shall ever remain grateful to him.

I would like to thank Mr. P.N. Mishra, Mr. Vishwakarma, Mr. Gujral, Mr. Sushil and Mr. A. Tariq for their invaluable help and cooperation they gave to me.

I would like to thank my friends, Shobhit, Jaine, DT, Madhup, Nano, Salil, Amit, Sirji, Rahul, PK, and Suneet for their warm affections and help to make my stay at IITK a pleasant one. I would also like to thank Shobhit, Jaine, and Suneet for coming to my rescue during the final stage of the thesis.

Lastly I express my deepest gratitude to my parents, my brother, bhabhi, and my sister for their invaluable support and affection.

Alok Tripathi
I.I.T.
Kanpur
August, 1999

Contents

Abstract

In the present study, the coil springs were tested experimentally, to know their heat transfer and friction characteristics. The coil springs were inserted in the smooth tube of internal diameter 16.5 mm and length 600-mm. The data were taken in the range of 2400<Re<9000. Test section was subjected to a uniform heat flux and was preceded by a developing length of 140×diameter brass tube. Temperatures at different locations were measured using Copper-Constantan thermocouples. Pressure drop and flow-rates were measured using inclined tube manometers. Both heat transfer augmentation and associated friction factors were calculated. Fractional increase in Nusselt number, friction factor and augmentation efficiency were calculated and compared with those for flow through the smooth tube. For the range of Re used, the efficiency of tube with springs was found to be lower than that for the twisted tapes and spirally fluted geometries, but it was found to be higher than that of mesh inserts, brush inserts, disks and stream line shapes.

List of Symbols

A	Cross-sectional flow area, m^2.
A_S	Heat transfer surface area, m^2.
C_p	Specific heat of the fluid, $J/kg-K$.
D_i	Maximum internal diameter of the tube, m.
f	Fanning friction factor.
$f(et)$	Fanning friction factor of enhanced tube.
$f(st)$	Fanning friction factor of smooth tube.
h	Heat transfer coefficient, W/m^2-K.
k_b	Fluid thermal conductivity at T_b, $W/m-K$.
L	Length of the test section, m.
$\dot{m}$	Mass flow rates, kg/s.
Nu	Nusselt number.
Nu_x	Local Nusselt number at location, x, from one end.
$Nu(et)$	Nusselt number of enhanced tube.
$Nu(st)$	Nusselt number of smooth tube.
Pr	Prandtl number.
ΔP	Pressure drop across the test section. Pa.
q	Input heat flux, W/m^2.
Q	Heat transferred to fluid per sec, W.
Re	Reynolds number.
Ta_o	Bulk air temperature at the outlet of the test section, °C
Ta_i	Bulk air temperature at the inlet of the test section, °C
Ta_x	Bulk air temperature at the location x, °C
T_b	Bulk air temperature, °C
Tw_x	Wall temperature at the location x, °C

Greek Symbols

μ	Dynamic viscosity, $kg/s-m^2$
ρ_c	Density of the manometric fluid, kg/m^3
ρ_a	Density of air, kg/m^3
η	Efficiency index

Subscripts

i	Conditions at inlet to test section
o	Conditions at outlet to test section
x	At the axial position x

List of figures

List of Tables

Chapter 1

INTRODUCTION

1.1 What is heat transfer augmentation?

The process of improving the performance of a heat transfer system is referred to as heat transfer augmentation, enhancement or intensification.

The augmentation heat transfer is a very important area of research. This is because, in recent time urgency has been felt to conserve energy and to stop environmental degradation, which is possible when high performance heat transfer equipments are used. The importance of this topic can also be judged from the fact that a large number of publications in several journals are devoted to this topic.

1.2 Application of heat transfer augmentation:

Heat Transfer Augmentation is applicable to those industries or places where the heat transfer systems are present. For example, Heat Exchangers are one such system. Heat Exchangers are used in a very large number of engineering applications. Be it a power generation industry, aerospace industry, or chemical industry, their application is a necessity. A large number of enhancement technologies have been developed to improve the performance of heat exchangers. Because of the applicability of heat transfer augmentation to heat exchanger that it has application not only in the traditional industries like steel, power generation and refrigeration, but also in modern industries like computer, aerospace and nuclear power.

1.3 Enhancement Techniques in Tube flow:

Augmentation techniques are divided into 2 groups: 'passive techniques' and 'active techniques'. Passive techniques employ special surface geometries. The active techniques require external power such as electric or acoustic fields and surface vibration.

1.3.1 Passive techniques:

Principle:

When fluid flows through a pipe, a thin boundary layer develops near the wall of the tube. It is this boundary layer that provides resistance to the heat transfer. If by using some device this boundary layer is destroyed, the heat transfer is enhanced. Passive techniques work on this principle. The following list briefly describes the passive techniques:

- Coated Surfaces: Examples include a non-wetting coating, such as Teflon. Surface coating promotes condensation and nucleate boiling etc.

- Surface roughness: Surface roughness increases the turbulence in flow, which results in heat transfer augmentation. This roughness is produced by many processes including internal knurling or threading, inserting rings of various types, inserting thin wire spirals, which are in good contact with the tube wall, and spirally grooving the tube etc.

- Internally finned tubes: Internal fins not only disturb the flow but also increase the surface area available for heat transfer augmentation.

- Displaced promoters: This includes mesh inserts, static mixer elements, rings or disks.

- Swirl flow devices: These devices create secondary swirling flow in the main flow, which results in enhancement of heat transfer. They include full-length twisted tapes, axial core inserts with screw type windings, and in-line propellers.

- Coiled tubes, which may provide a very compact heat exchanger.

- Surface tension: These devices use surface tension forces to drain the liquid films.

- Besides all the above mentioned devices some additives can also be added in liquids and gases which increase the surface area for heat transfer enhancement.

1.3.2 Active Techniques:

Principle:

If the flow is stirred by means of some external device, the turbulence is increased in the flow. As a result, heat transfer is enhanced. There are various active techniques like –

- Rotating the surface by some mechanical aid.
- Surface vibration.
- Fluid vibration.
- Electrostatic field can be directed to cause greater bulk mixing of fluid.
- Injecting the fluid to disturb the boundary layer or sucking it so as to remove it.

1.4 Objective of the present study:

A number of studies have been conducted on a wide range of enhancement goemetries. Still the researchers are trying to find out some other devices to investigate their heat transfer enhancement characteristics. The present work, with a helical coil spring in a circular tube, is a step in that direction.

In the present experimental analysis, constant heat flux conditions were used to determine the performance of the enhancement device. The working fluid is air.

The overall objective of the present work is:

- To carry out an extensive experimental investigation of pressure drop and heat transfer with a smooth tube and tube with helical coil springs inserted in the tube.
- Comparison of results for an enhanced tube with those for a smooth tube to assess the performance of spring as an augmenting device.
- Variation of heat transfer and friction factor characteristics of spring with its pitches.

Chapter 2

LITERATURE REVIEW

A number of geometries have been tested to find out how much enhancement of tube side convective heat transfer has taken place. So far the work in this area has been mostly experimental. The mathematical modeling has not been able to predict the heat transfer and pressure drop correctly for any of the augmenting geometries.

Extensive investigation has been done on twisted tape inserts for both laminar as well as turbulent flows. Date and Singham (1972) considered a circular tube with twisted tape insert subjected too axially constant wall heat flux. They showed that the Nusselt Number was dependent upon 4 groups of parameters as given below:

$$Re_d / X_L,\ C_{fin},\ P_r \text{ and } X_L$$

Where, $C_{fin} = K_m \delta / K_f d$

K_m = Thermal conductivity for tape material

X_L = H (Pitch) / d (dia of tube)

Date (1974) analysis showed that Nusselt Number increased by increasing the Prandtl Number and the Reynolds Number and by decreasing X_L. They also correlated their numerical results within $\pm 5\%$ as,

$$(f\,\mathrm{Re})_d = 38.4(\mathrm{Re}_d / X_L)^{0.05} \qquad 6.7 \le \mathrm{Re}_d / X_L \le 100$$

$$C(\mathrm{Re}_d / X_L)^{0.3} \qquad \mathrm{Re}_d / X_L > 100$$

Hong and Bergles (1976) also experimentally determined the friction factor for a twisted tape fully developed flow using ethylene glycol and water as test fluids. They correlated their test results by following expression

$$Nu_d = 5.172\{1 + 0.005484[\Pr(\mathrm{Re}_d / X_L)^{1.78}]^{0.7}\}^{0.5}$$

Gupta and Date (1989) tested 3 tape geometries in an annulus with air as the test fluid. A semi analytical model was developed by them, which predicted the friction data reasonably accurately.

Saha et al. (1989) conducted an extensive experimental programme on segmented twisted tapes in laminar flow of water with constant heat flux. They proposed a series of rather complex empirical correlations to predict the Nusselt number and friction factor as a function of Re, Y, Z,

Where, Y: twist ratio and Z: dimensionless pitch

Agrawal and Rao (1996) conducted experiments to evaluate friction and heat transfer characteristics of twisted tapes for heating and cooling of Servotherm oil (medium grade) under uniform wall temperature condition within $70 \leq \mathrm{Re} \leq 4000$ and $195 \leq \Pr \leq 375$. Correlations were also developed for the prediction of Friction Factor and Nusselt Number. Several other geometries have been studied which are summarised in Tariq (1999) and given here in table (2.1).

Betal (1989) reported data for 3 propellers placed in a staggered manner in fully developed flow of water through a pipe subjected to constant heat flux.

Chaturvedi and Kant (1992) also conducted experiments with in-line propellers placed in fully developed flow of water through a pipe in the Reynolds number range of $16000 < \mathrm{Re} < 68000$. Results showed that the maximum augmentation in heat transfer was obtained at the interpropeller distance of 9.72D (where D was the internal diameter of the tube) and Re = 45000.

Table 2.1

Comparison of Heat Transfer Coefficient Augmentation with Various Augmentation Devices under their Best Operating Conditions.

Promoter	Exp. Conditions	Re	Nu_i	F_i/f_s	η
Twisted tapes (Laminar) Honk and Bergles (1974)	For water in 1.02 cm i.d. tube with 0.97 cm wide twisted tapes of pitch to dia ratio of 2.45	100 2000	1.3 8.5	11.5 11.5	0.74 to 0.11
Twisted tapes (Turbulent region) Smithberg et.al. (1964)	For water in 3.51 cm i.d. tube with 3.48 cm wide twisted tapes of pitch to dia ratio of 3.62	20,000 50,000	3.5 3.5	2.5 2.0	1.5 to 1.4
Wire coils Krieth et. Al. (1959)	For water in 1.35 cm i.d. tube with close fitting wire coils of pitch to dia ratio of 1.77	10,000 10,000	3.2 3.4	6.8 4.8	0.71 to 0.47
Mesh inserts Megerlin et.al. (1974)	For water in 0.53 cm i.d. tube with close fittings s.s. mesh inserts of 80% porosity.	10,000 to 30,000	9.0	55.0	0.16
Brush inserts Megerlin et. Al. (1974)	For water in 0.53 cm i.d. tube with close fitting s.s. brushes	10,000 to 30,000	5.0	35.0	0.09
Disks Evans and Churchill (1962)	For water in 2.55 cm i.d. tube with disks of 2.33 cm dia at spacing of 12 dia	10,000 50,000	2.5 2.0	75.0 100.0	0.04 to 0.02
Promoters Thomas (1967)	Cm i.d. tube with 1.91 cm o.d. and 1.57 i.d. rings spaced 0.64 cm apart	30,000	1.9	12.5	0.15 to 0.03
Streamline shapes evans and Churchil (1962)	For water in 2.55 cm i.d. tube with streamline shapes of 2.23 c.m dia at a uniform spacing of 12 tube dia	10,000 5,000	2.2. 1.7	35.0 40.0	0.06 to 0.04
Static Mixers Lin et. Al. (1977)	For R133 in 1.27 cm i.d. tube with close fitting static mixers of pitch to dia ratio of 1.5	1,000 5,000	6.0 10. 0	3.0 4.6	2.28 to 2.0
Propeller type baffles (static) colburn et al. (1931)	For air in 6.67 cm i.d. tube with baffles spaced uniformly 7.62 cm apart.	25,000 to 150,000	3.4	40.0	0.09
In-line Propellers Betal (1989)	For water in 5.0 cm i.d. tube with 3 in-line propellers placed staggeredly.	4,000 to 10,000	1.1 to 2.0	3.5 to 4.7	0.5
In-line propellers Chaturvedi an Kant (1992)	For water in 5.0 cm i.d. tube with 5 in line propellers spaced 9.72 D apart	40,000 to 55,000	6.0	4.0	2.5

Khanna and Kant (1994) showed that the efficiency with 3 in line propellers placed in fully developed flow of air through the pipe was greater than that with the mesh inserts, brush inserts, disks, and streamline shapes, but lower than that for the twisted tapes.

Marto et al. (1979), Yampolsky (1983, 1984) and Panchal & France (1986) have tested several spirally fluted tubes. The data showed an increase of 50-300 % in heat transfer relative to smooth tube while negligible change in corresponding friction factor. Lu Cheng et al. (1994) has tried to explain the underlying causes for this highly desirable behavior of spirally fluted tube. They claimed that it was especially high Prandtl number mixing that was enhanced by passage through spirally fluted tubing.

Obot et al. (1992) did an extensive experimental investigation on 23 commercially available enhanced passages. The internal surfaces of all enhanced passages had spirally shaped geometries as shown in Fig (2.1). The test conditions for the flow is given in table (2.2).

Panchal & France (1993) tested spirally indented tubes for heat exchanger applications with water as test fluid in the Prandtl Number range of $3.6 \leq Pr \leq 8.8$.

Fu & Tseng (1994) studied numerically the heat transfer in a heated circular tube with an inner tube inserted. Calculations were performed for Reynolds numbers of 100, 500 and 1000 and Prandtl numbers of 0.1, 0.7, 7.0 and 10.0. The results showed that except at very low Peclet Number the heat transfer rate of heated tube was increased when an inner tube was inserted.

A recent experimental investigation was done by Jensen & Vlakancic (1999) on internally finned tubes with water as test fluid. They studied both micro-finned tubes as well as high finned tube and developed the correlations for the Nusselt number and friction factor. They showed that the effect of various parameters on heat transfer augmentation and pressure drop was not same for micro finned tubes and high finned tubes. They showed, for example, that the heat transfer augmentation was

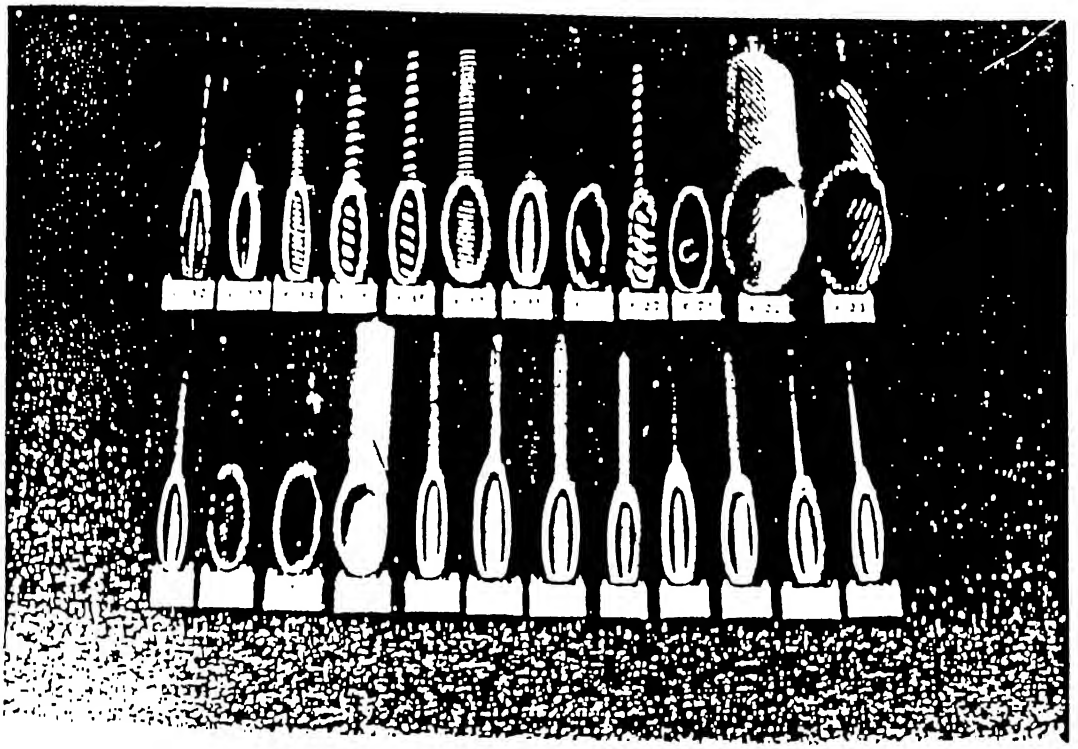

Fig 2.1

Photographs of surface contours for different passages.

TABLE 2.2Test Conditions for the Flow Passages.

Tube	D_i (mm)	L_e (mm)	$L_{e,r}$ (mm)	L_h (mm)	L_p (mm)	A_h (mm^2)	A_z (mm^2)	L_e/D_i	$L_{e,r}/D_i$	L_h/D_i	L_p/D_i
S-0	13.39	2019			381		140.8	150.8			
		1969		458.0	381	19266		147.1		34.2	28.5
					1565.3		361.4				73 0
GA-1	21.45	254			1354.1			11.8			63.1
		1016			920.8			47.4			42.9
GA-2	23.96				1587.5		450.9				
		254			1343			10.6			56.1
		254			2773.4			8.9			97.3
GA-3	28.49	1089			920.75			38.2			32.3
		1089	38.1		838.2			38.2	1.3		29.4
			1524	381.0	304.8	34101	637.5		53.5	13.4	10.7
HC-4	13.87		1968.5	441.1	365 0	19221	151.1		141.9	31.8	26.3
HC-5	17.78		1968.5	344.2	268.0	19224	248.3		110.7	19.4	15.1
HC-6	17.61		1968.5	347.5	271.3	19224	243.6		111.8	19.7	15.4
W-7	14.10		1165.2	434.1	357.9	19229	156.2		82.7	30.8	25.4
W-8	14.40		1968.5	424.9	348.7	19224	162.9		136.7	29.5	24.2
W-9	15.90		1644.7	384.8	308.6	19222	198.6		103.4	24.2	19.4
W-10	14.95		2087.6	410.5	333.5	19278	175.5		139.6	27.4	22.3
W-11	14.45		2089.2	423.4	347.2	19222	164.0		144.6	29.3	24.0
W-12	14.56		2133.6	420.4	344.2	19228	166.5		146.6	28.9	23.7
W-13	14.45		2133.6	423.4	347.2	19222	164.0		147.6	29.3	24.0
Y-14	12.68		1651	482.9	406.7	19227	126.2		130.3	38.9	32.1
Y-15	19.16		1651	319.6	243.4	19231	288.2		86.2	16.7	12.7
Y-16	19.53		1651	313.3	237.1	19223	299.6		84.5	16.0	12.1
Y-17	24.22		1651	448.6	372.4	34131	460.7		68.2	18.5	15.4
Y-18	18.81		1651	325.3	249.1	19224	277.9		87.8	17.3	13.2
Y-19	22.88		1651	474.5	398.3	34110	411.2		72.2	20.7	17.4
Y-20	16.05		1651	381.2	330.4	19223	202.3		102.9	23.8	20.6
Y-21	23.45		838.2	463.1	386.9	34113	431.7		35.8	19.8	16.5
Y-22	48.65		522.3	457.2	381.0	69878	1859		10.7	9.4	7.8
Y-23	47.67		1622.4	466.5	390.2	69855	1785		34.0	9.8	8.2

increased by increasing the number of fins for high finned tubes while it was insensitive for micro finned tubes.

Ravigururajan and Bergles (1995) obtained experimental data for in-tube flow of low temperature water to understand the characteristics of internally enhanced tubes for small e/d ratio of 0.2 and less. They also established the optimum description design parameters for different Prandtl Numbers.

Numerical studies on flow through the spirally indented tubes were also done by Kalnin (1974), Withers (1980 a, b), Li et al. (1982), Yorkshire (1982), Ravigururajan & Bergles (1985, 1986) and Bergles (1986). They presented statistical correlations that could be used independently to evaluate friction factor and heat transfer coefficient. Wither's correlations overpredicted the friction factor and deviation increased to over 50 % with increasing indentation height beyond 0.038D (D:diameter of the tube). Li's correlations did not predict correctly for the small indentation height. The best prediction was done by the Bergles' correlation. Similarly heat transfer coefficient due to Wither and Li were not predicted correctly for large pitches. Wither's equation overpredicted the heat transfer coefficient while Li's equation underpredicted the data, though both correlations predicted data trend reasonably well.

Dolata (1984) studied the augmentation of heat transfer between fluid stream and tube wall by embedded perforated baffles. The work revealed that the enhancement of heat transfer could be predicted with reasonable accuracy by a simple correlation as,

$$Nu = 0.34(\mathrm{Re}^{+})^{0.698}(\mathrm{Pr})^{0.4}$$

$$\text{Where, } \mathrm{Re}^{+} = \mathrm{Re}(\xi/8)^{1/2} \text{ and } \xi = \frac{2\Delta P D}{\rho U^{2} L}$$

Besides the circular tube, heat transfer enhancement for the non-circular ducts with a fluid flowing through it has also been studied. Kostic (1994) reviewed the current knowledge on fluid mechanics and heat transfer of non-Newtonian fluids in rectangular or square ducts. He proposed that fluid elasticity might be the major factor

for the laminar heat transfer enhancement in non-Newtonian fluids in non-circular duct flow.

Lin et al. (1996) investigated the laminar flow heat transfer enhancement in a small-scale duct with Aqueous Carbopol solutions. He showed that enhanced heat transfer behavior of the Carbopol solution within low Reynolds number range is different from that within relatively high Reynolds number range. He also showed that there exists a limiting polymer concentration, Cmax at which the non-Newtonian fluid possesses the maximum ability to enhance the heat transfer. Besides this the effect of various geometrical parameters such as, duct shape, rib height etc. were studied by many researchers like Chandra & Han (1989), Chyn & Wu (1989), Taslim et al. (1991), Archrya et al. (1993), Liou & Hwang (1993) and Taslim & Wadsworth (1994).

Chapter 3

THE EXPERIMENTAL DESCRIPTION

3.1 Introduction

As mentioned in previous chapter, a number of surface geometries have been tested for augmentation of heat transfer in different ranges of Reynolds Number. In each case the objective has been to assess as how much heat transfer has been increased and how much is the increment in pressure drop? As per our knowledge coil springs of varying pitches have not been tested so far. The coil springs are easy to manufacture and in many cases are available in market. They are also easily reproducible geometries. That is why they were selected as augmenting surface geometries in the present investigation.

3.2 Dimensions of coil springs:

In the experiment air was blown through a brass tube of internal diameter 16.5 mm and length 600-mm. The coil springs were such that they just touched the internal surface of the tube. Thus the external diameter of each coil spring was very close to 16.5 mm within the tolerable limit so that it can easily enter inside the tube. The length of each spring was 600 mm. Four springs were used with pitch 4 mm; 9 mm, 15 mm, and 42 mm to know the dependency of heat transfer on pitches. The maximum pitch depended on the limitations in manufacturing the springs. Special order was placed to manufacture these springs.

3.3Test Unit:

Test section was a brass tube of internal diameter 16.5-mm, external diameter 22.0 mm and length 600 mm. Air from a compressor was blown through it. This test section was preceded by another brass tube, which had its internal diameter 16.5 mm and length 2500 mm. This longer tube was fitted to the test section so that the flow became fully developed at the entrance of the test section. The developing length was calculated on the basis that, for flow through a pipe the developing length is equal to the 140 times the diameter of the pipe.

Twelve equispaced axial locations were chosen on the top surface of the test section to measure the temperature. Further at each location temperature was measured on 2 circumferentially opposite points. Small grooves (about 1.25 mm deep) were made to place the thermocouple beads properly.

The test section and developing length were joined by 2 brass flanges. A thick gasket seal (about 20 mm thick) was sandwiched between the 2 flanges. This was done to avoid the air leakage and also to minimize the heat loss by longitudinal conduction through the brass.

How the thermocouples were set?

First the thermocouple beads were placed in grooves in such a manner so as to ensure their surface contact with the groove surface. After that thermocouples were wound tightly with G.I. wire and cello tape so as to ensure that it did not get displaced from its location.

3.4 Experimental Set- Up:

3.4.1 General Description

The experimental set-up is shown in Fig 3.1. The compressed air was provided by an air compressor. To ensure the constant flow rate a pressure regulator was fitted just at the compressor exit. Air, then flew through a brass tube of 16.5-mm internal diameter and 2500 mm length. Thus a hydrodynamically developed flow was achieved at the entrance of the test section. The test section was subjected to a constant heat flux. The uniform heating was achieved by A.C. current from a stabilized single phase variable voltage transformer to the flexible heating tape (covered by U.K. Patent No. 668163) which was wound uniformly over the entire test section. The test section was insulated using glass wool. Aluminum foil was wound over the test section to avoid the heat gain from outside. To measure the voltage applied across the heating tape and current passing through it a digital voltmeter and an ammeter were used respectively. For selecting the suitable voltage and wattage, the company-supplied nomogram was used. It indicated the maximum voltage that can be applied across the heating tape without causing any damage to it.

3.4.2 Thermocouple Specification:

Copper – Constantan Thermocouple supplied by Love Controls Corporation U.S.A were used. These thermocouples were initially calibrated using the constant temperature bath of silicone oil with an accurate standardized Hg-in glass thermometer.

3.4.3 Temperature Measurement

All the thermocouples were connected to a temperature measuring instrument (THERM – 3280 – 6M, Nr T [illegible] m 220 V/50 Hz German

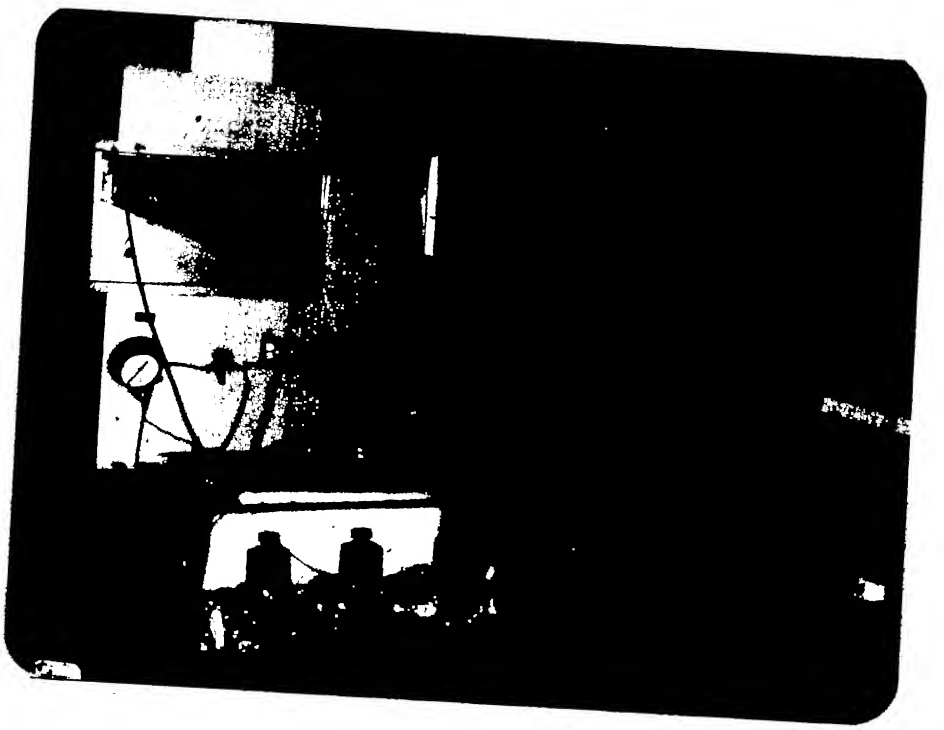

Fig 3.1(a) Photograph of Experimental Rig.

Fig 3.1(b) Photograph of helical coil springs used as augmenting devices

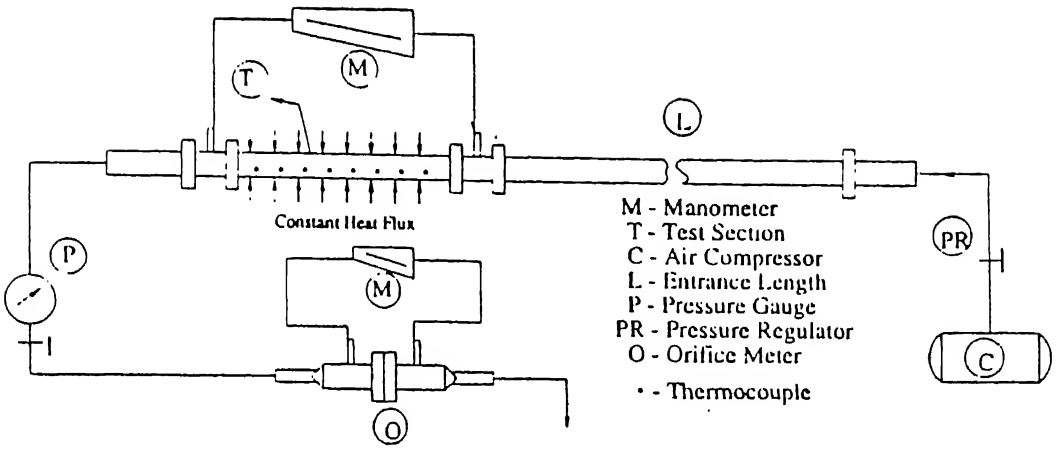

Schemetic Diagram of Test Rig.

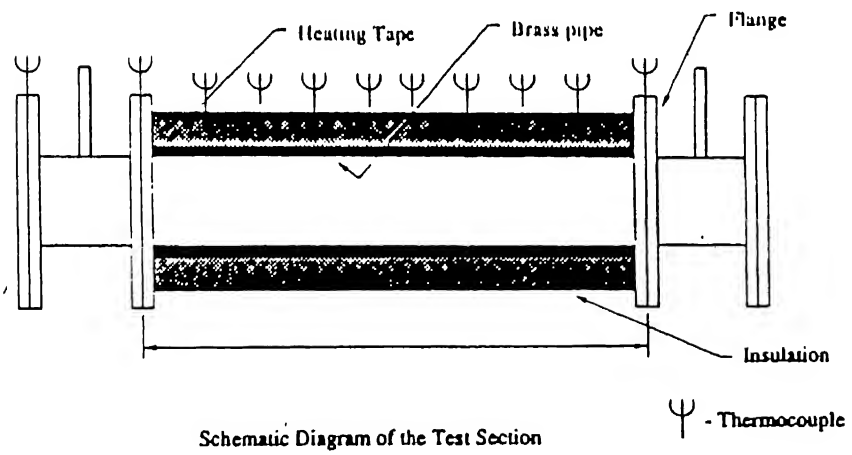

Schematic Diagram of the Test Section

Figure 3.2

Make) through selector switches. By changing the position of knob on selector switch we get the temperature (in °C) as measured by different thermocouples. A total of 26 thermocouples were used. Two of them were used to measure bulk air temperature at the inlet and outlet of the test section. Rest 24 thermocouples were used to measure wall temperature of the tube. As mentioned earlier, at each axial location 2 thermocouples were fixed at circumferentially opposite points. This was done to minimize the error in temperature measurement.

3.4.5 Measurement of Pressure drop across the test section

To measure the pressure drop across the test section 2 types of inclined tube manometers were used. In case of smooth tube, the pressure drop across the tube was very small. Therefore, a manometer was needed which could measure accurately even a very low pressure drop. So an inclined tube manometer with manometric fluid of specific gravity 0.826 having a range of 0 to 0.1 inch of H_2 O was used. However, when the coil springs were inserted inside the tube, the earlier manometer was not able to measure the pressure drop as it shot beyond the range of the manometer. Hence, another inclined tube manometer of higher range had to be used; it had distilled water as the manometric fluid (specific gravity 1.000).

3.4.6 Measurement of Flow Rate

To measure the flow rate, an orifice meter was used. Flow rate was measured in terms of pressure drop across an orifice plate. Readings were taken using an inclined tube manometer with manometric fluid of specific gravity 0.826. The orifice meter was calibrated prior to the measurements using the calibration chart.

3.4.7 Experimental Procedure

The steps involved in performing the experiment were as follows:

1). The compressor was switched on and the pressure regulating valve was opened to get the desired flow rate.

2). A suitable voltage across the heating tape was applied using a variac.

3). Steady state was obtained approximately after an hour. Then the readings for the temperature and pressure drop were taken.

4). In a similar way each time flow rate was increased and data were recorded. It is worthwhile to mention that steady states for the second and subsequent flows were obtained after time intervals of 15 minutes.

5). Once the experiment with smooth tube was over, the flanges from the exit side of the test section were removed and spring was inserted inside the tube. Flanges were again fitted and all the above mentioned steps were repeated.

6). Similarly the experiments were conducted for other springs.

Chapter 4

RESULTS AND DISCUSSION

This chapter is divided into 7 sections. First section consists of the assumptions involved in evaluating Nusselt number and friction factor. Second section deals with the complete procedure for evaluating Nusselt number. Computation of friction factors is discussed in the third section. In next section experimental data obtained for smooth tube have been compared with the published data. Fifth section analyzes the data and evaluates the spring as an augmenting device. Conclusions from the study are given in sixth section. Last section suggests some of the future work that may be carried out in this direction.

4.1 Assumptions

1. The thermocouples fixed to the test section at various locations measure the outside wall temperature. Since the thickness of tube is small and conductivity of brass is sufficiently high, therefore there will be a minute difference (0.02^0C as calculated considering one dimensional steady state conduction) between outside wall temperature and inside wall temperature. This difference has been neglected and for all calculation purposes, inside wall temperature has been taken as the outside wall temperature.

2. Since the temperature increase of air from inlet to outlet was not very high, it has been assumed that the temperature of the fluid at a particular location in the test section, i.e. Ta_x, varies linearly from the inlet to the outlet of the test section.

4.2 Calculation of Nusselt number

4.2.1 Procedure for calculating Nusselt number

As mentioned earlier, temperatures at twelve locations along the length of test section were measured. At a particular position, temperatures were measured on two circumferentially opposite points. The steps involved in calculation of Nusselt number are narrated in sequence below :

1. Average temperature (Tw_x) at each location is calculated taking mean of two temperatures measured at two circumferentially opposite points.

2. Using the inlet and exit air temperatures and assuming linear variation (as mentioned above), the bulk air temperatures (Ta_x) at various locations were calculated.

3. Mass flow rate was calculated by using the following formula

$$\dot{m} = \frac{C_d}{\sqrt{1-\beta^4}} A_t \sqrt{2\rho_a(\Delta P)} \qquad kgs^{-1} \tag{4.1}$$

where, β = 0.6 (diameter ratio)

A_t = $(\pi/4)d^2$, d : diameter of orifice meter = 15 mm

ρ_a = density of air

C_d = coefficient of discharge

= 0.755 for the orifice used in our experiment

ΔP = $\rho_c g h_c$, (ρ_c = density of manometric fluid)

h_c = reading of inclined tube manometer

Here ρ_a was calculated at T = 308 ° K

4. Using flow rate m, Reynolds Numbers were calculated as follows

$$\mathrm{Re} = \frac{4\dot{m}}{\pi d\mu} \tag{4.2}$$

where,

μ = dynamic viscosity

d = envelope diameter

It should be noted that diameter of an enhanced tube can be expressed in many ways. In this thesis, maximum diameter of the enhanced tube was taken to be the enveloped diameter, as suggested by Marner et al. (1983). Here d = D_i (internal diameter of the tube).

5. Local Nusselt Number at any location x is given by

$$Nu_x = \frac{hD_i}{k_b} = \frac{qD_i}{k_b(Tw_x - Ta_x)} \tag{4.3}$$

where, q (heat flux transferred to the fluid) = Q/A_S

In ideal condition this heat Q must be equal to the total heat supplied by heating tape. However because of various losses involved the heat supplied by heating tape was not equal to the net heat carried away by the fluid. Therefore here in all calculation Q is taken as the heat carried away by the air. i. e.

$$Q = \dot{m}C_p(Ta_o - Ta_i) \tag{4.4}$$

Hence,

$$Nu_x = \frac{mC_p(Ta_o - Ta_i)D_i}{A_S k_b(Tw_x - Ta_x)} \tag{4.5}$$

Where,

$\dot{m}$ = mass flow rate of air

C_p= specific heat of air calculated at mean temperature $(Ta_i + Ta_o) / 2$

D_i = internal diameter of the tube

A_S= inner surface area of the tube

k_b = thermal conductivity of the fluid at mean temperature $(Ta_i + Ta_o) / 2$

The variation of the Local Nusselt Number for different Reynolds Numbers with respect to axial positions along the length of the tube are tabulated in Tables 4.1 to 4.5. Their plots are given in Figs. 4.1 to 4.10.

6. The average Nusselt Number for a particular flow rate was calculated by integrating the local Nusselt Number over entire length, L, of the test section using Trapezoidal rule as follows:

$$\overline{Nu} = \frac{1}{(x_2 - x_1)} \int_{x_1}^{x_2} Nu_x dx = [Nu_{125} + 2(Nu_{175} + Nu_{225} + Nu_{275} + Nu_{325} + Nu_{375} + Nu_{425}) + Nu_{475}] \frac{h}{(x_2 - x_1)} \quad \textbf{(4.6)}$$

where,

$h = 50$ mm

$x_2 - x_1 = 475 - 125 = 350.$

The average Nusselt Numbers are given in Table 4.6 and plotted in Fig.4.11.

4.2.2 Sample Calculation:

Calculation of Nusselt Number at x = 125 mm:

$$Ta_i = 34.7^{\circ} C$$

$$Ta_o = 65.0^{\circ} C$$

Table 4.1: Local Nusselt number variation with axial distance x for different Reynolds number (for smooth tube)

Axial position along the length of the tube (x) in mm	Local Nusselt Number (Nu) at different values of Reynolds Number (Re)									
	Re = 2400	Re = 3400	Re = 4167	Re = 4823	Re = 5363	Re = 5903	Re = 6366	Re = 7215	Re = 7948	Re = 8643
25	13.60	20.58	26.01	30.58	34.50	37.62	40.23	43.01	48.45	50.27
125	8.07	11.81	14.94	17.53	19.61	21.59	23.15	25.58	28.86	29.68
175	6.58	9.62	12.11	14.24	15.83	17.47	18.41	20.23	22.72	23.41
225	7.12	10.55	13.49	16.06	18.33	20.26	21.60	24.24	27.83	28.29
275	7.78	11.55	13.83	17.63	19.81	22.02	23.46	26.16	29.73	30.33
325	8.42	12.54	16.23	19.51	22.17	24.66	26.20	29.42	33.15	33.33
375	8.67	12.92	16.88	20.31	23.17	25.92	27.36	30.44	35.72	36.02
425	8.56	12.34	15.76	18.84	21.24	23.27	25.03	27.75	29.99	29.79
475	9.56	13.78	17.26	20.59	22.91	25.14	26.71	29.42	32.07	31.47
525	20.08	30.41	39.39	49.94	55.82	63.94	66.25	73.21	83.47	79.23
575	31.77	46.21	58.45	80.98	90.29	104.68	103.97	104.27	130.71	118.16

Table 4.2: Local Nusselt number variation with axial distance x for different Reynolds number (for tube having spring of pitch 4mm.)

Axial position along the length of the tube (x) in mm	Local Nusselt Number (Nu) at different values of Reynolds Number (Re)									
	Re = 2400	Re = 3400	Re = 4167	Re = 4823	Re = 5363	Re = 5903	Re = 6366	Re = 7215	Re = 7948	Re = 8643
25	13.06	20.53	27.40	31.88	35.50	40.69	45.44	55.56	62.56	68.70
125	8.36	12.69	17.44	20.39	22.95	26.24	29.32	34.82	41.20	45.23
175	6.94	10.44	14.06	16.17	18.15	21.19	22.95	26.95	31.85	34.63
225	7.99	12.31	17.31	20.08	22.53	25.87	29.63	35.77	42.77	49.64
275	9.03	14.04	19.79	22.46	25.31	29.16	32.95	40.02	48.35	53.60
325	9.72	15.07	21.56	25.10	27.83	31.70	36.40	44.24	53.66	60.05
375	10.02	15.71	22.59	25.59	29.31	34.00	39.39	48.13	57.91	66.50
425	9.21	13.78	19.41	21.37	24.10	27.45	30.59	36.44	43.10	46.70
475	10.29	15.42	21.98	23.76	26.70	30.14	33.71	42.36	48.16	52.53
525	22.27	34.46	61.56	61.18	70.70	85.65	100.77	130.02	163.65	187.04
575	34.63	60.17	147.59	100.43	115.23	146.56	172.01	250.22	331.62	511.30

Table 4.3: Local Nusselt number variation with axial distance x for different Reynolds number (for tube having spring of pitch 9mm.)

Axial position along the length of the tube (x) in mm	Local Nusselt Number (Nu) at different values of Reynolds Number (Re)									
	Re = 2400	Re = 3400	Re = 4167	Re = 4823	Re = 5363	Re = 5903	Re = 6366	Re = 7215	Re = 7948	Re = 8643
25	16.77	28.36	35.03	41.01	46.15	48.59	54.85	62.60	70.95	77.46
125	11.27	18.85	23.90	27.18	30.97	32.42	38.94	45.22	48.49	50.80
175	9.29	14.81	18.77	21.15	24.49	25.18	30.19	34.73	38.13	41.13
225	10.70	18.07	23.44	27.05	31.65	33.52	40.80	46.96	53.58	58.22
275	11.58	19.26	24.80	27.85	33.79	35.31	43.68	50.53	57.19	62.81
325	12.56	21.42	27.90	32.31	38.29	39.78	50.79	58.14	67.22	75.26
375	12.70	21.35	28.26	32.69	39.07	41.12	51.94	62.61	72.99	80.60
425	11.25	17.73	22.85	25.93	30.65	31.22	39.86	44.94	52.84	58.67
475	12.43	19.72	25.34	28.41	33.54	34.47	45.11	51.59	57.62	64.33
525	36.97	49.04	70.95	79.98	101.01	99.40	163.23	197.99	264.24	319.11
575	37.43	66.94	98.06	111.66	151.84	145.46	298.09	366.29	547.34	1329.64

Table 4.4: Local Nusselt number variation with axial distance x for different Reynolds number (for tube having spring of pitch 15mm.)

Axial position along the length of the tube (x) in mm	Local Nusselt Number (Nu) at different values of Reynolds Number (Re)									
	Re = 2400	Re = 3400	Re = 4167	Re = 4823	Re = 5363	Re = 5903	Re = 6366	Re = 7215	Re = 7948	Re = 8643
25	14.91	23.14	28.30	31.98	34.64	37.89	40.65	46.54	51.27	56.76
125	9.91	15.90	20.48	23.76	26.49	29.88	32.01	37.68	41.30	46.97
175	8.11	12.96	16.32	19.36	21.24	23.56	25.61	32.76	33.95	36.96
225	9.14	14.71	19.13	22.51	25.55	28.73	31.08	36.58	40.64	44.26
275	9.78	15.69	20.48	24.64	27.46	31.01	34.11	40.95	45.07	49.82
325	10.27	16.81	21.99	26.44	29.22	34.79	36.59	43.49	48.08	50.15
375	10.58	17.22	22.68	27.26	31.40	36.44	39.81	47.33	50.41	55.62
425	9.47	14.52	18.53	21.85	24.23	27.98	30.44	35.19	38.56	42.09
475	10.41	16.41	20.34	24.00	27.29	31.01	33.91	40.05	41.47	45.27
525	20.98	32.88	42.23	50.29	56.71	64.79	70.82	75.45	90.62	98.40
575	32.31	50.17	62.77	72.55	88.82	106.18	116.64	119.60	126.50	117.75

Table 4.5: Local Nusselt number variation with axial distance x for different Reynolds number (for tube having spring of pitch 42mm.)

Axial position along the length of the tube (x) in mm	Local Nusselt Number (Nu) at different values of Reynolds Number (Re)									
	Re = 2400	Re = 3400	Re = 4167	Re = 4823	Re = 5363	Re = 5903	Re = 6366	Re = 7215	Re = 7948	Re = 8643
25	13.29	19.74	24.54	28.01	30.27	31.10	31.25	32.95	37.04	40.48
125	9.23	14.04	17.78	20.68	22.43	23.49	23.93	26.46	29.83	30.93
175	7.64	11.55	14.50	16.94	18.38	18.96	19.19	21.11	23.65	24.77
225	8.55	13.57	17.12	19.91	22.41	23.33	23.53	26.63	31.44	32.37
275	9.39	15.09	19.36	22.54	25.13	26.13	25.95	29.12	32.98	34.25
325	10.08	15.71	20.12	23.59	26.33	27.33	26.81	30.07	33.85	35.62
375	10.43	16.03	20.90	24.15	27.99	28.75	28.28	31.49	36.87	37.70
425	8.92	13.03	15.76	19.59	21.04	21.76	21.04	25.54	31.72	33.47
475	11.25	16.14	20.10	23.34	25.72	26.30	24.96	30.26	35.25	35.03
525	20.32	30.91	39.43	49.93	52.85	52.88	47.69	57.88	81.89	81.94
575	61.42	85.72	100.81	120.73	131.33	138.22	86.38	113.10	128.19	125.34

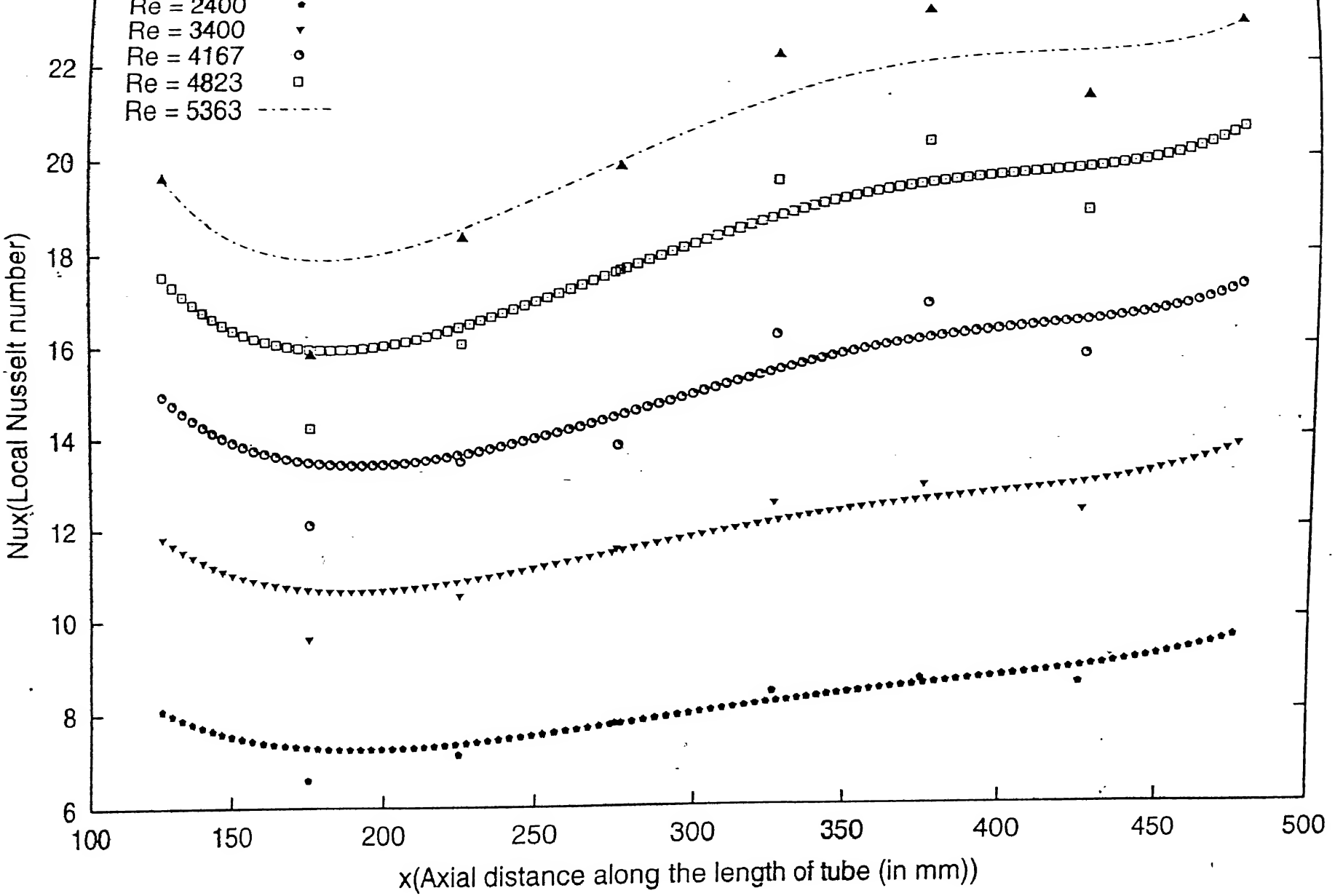

Fig 4.1:Nusselt number variation along the length of tube [Smooth Tube]

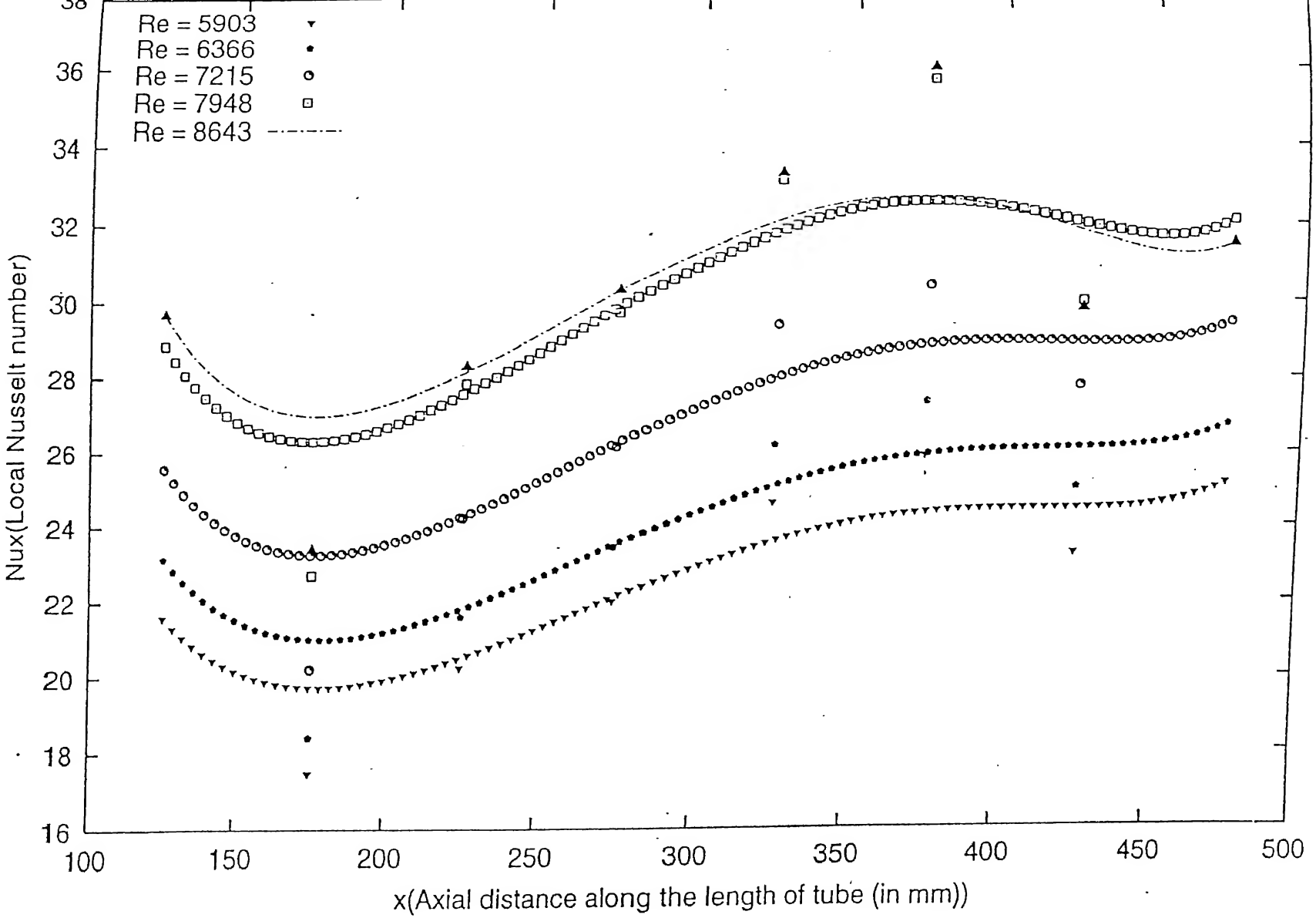

Fig 4.2:Nusselt number variation along the length of tube [Smooth Tube]

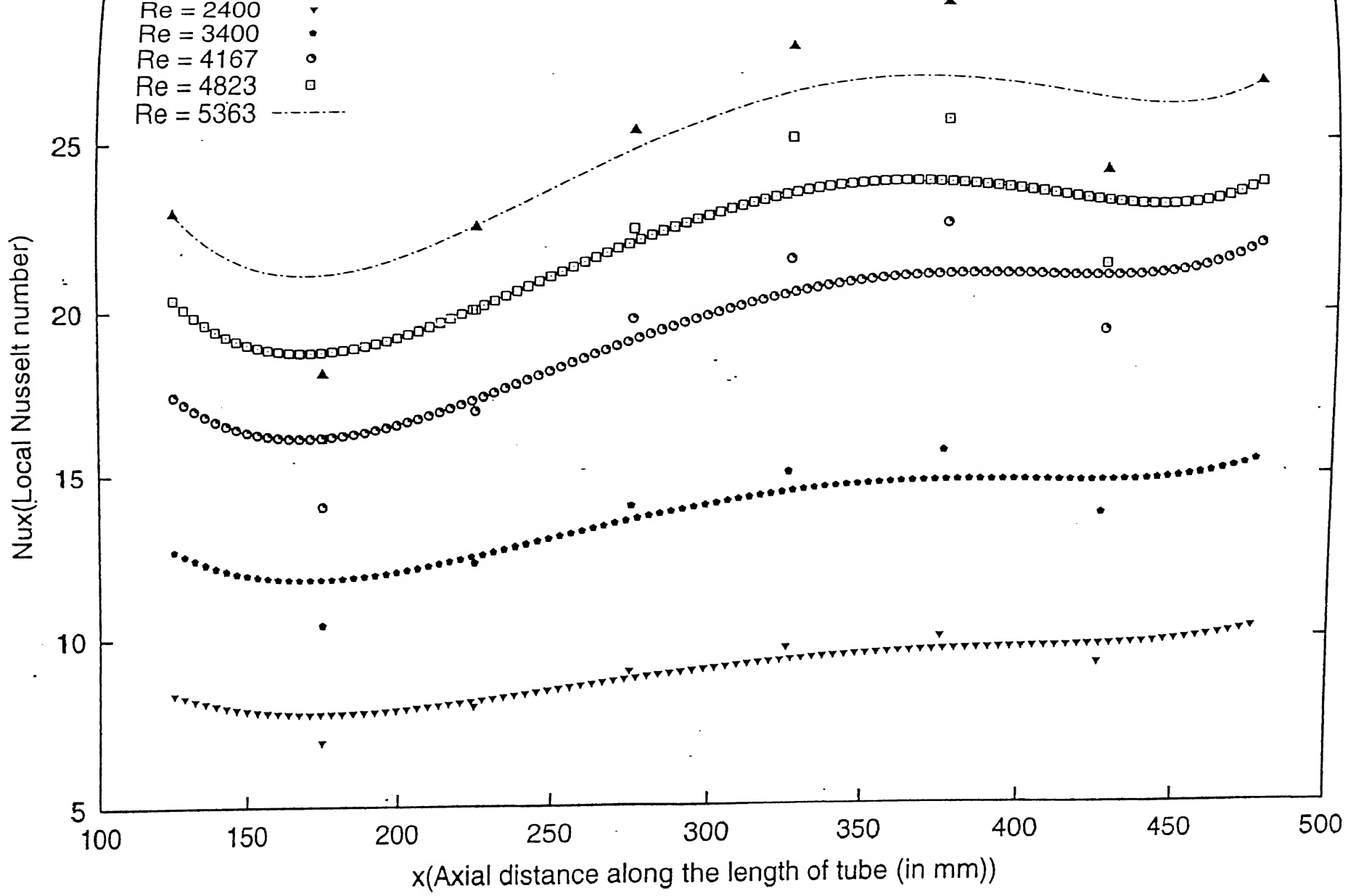

Fig 4.3:Nusselt number variation along the length of tube [with pitch 4 mm]

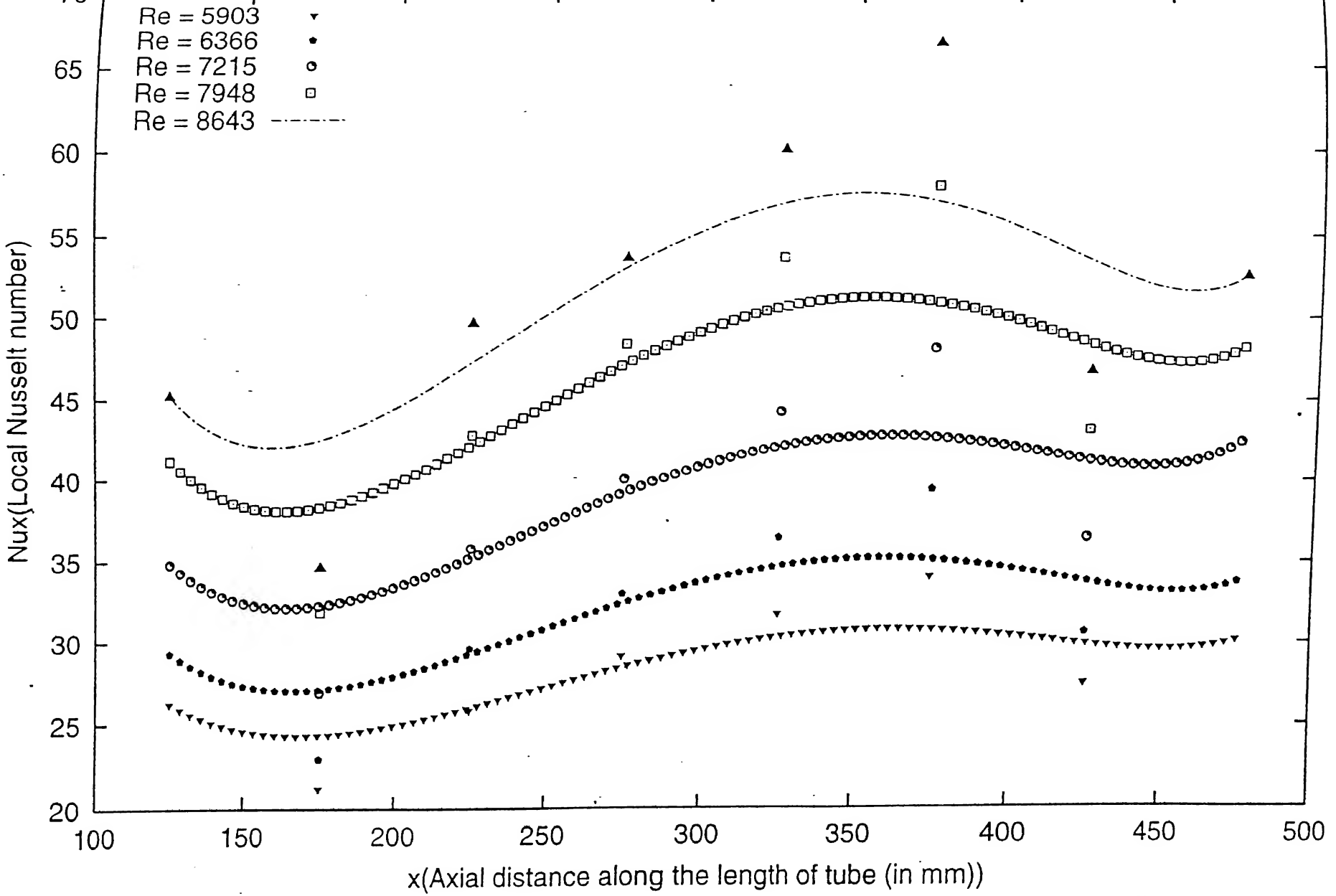

Fig 4.4:Nusselt number variation along the length of tube [with pitch 4 mm]

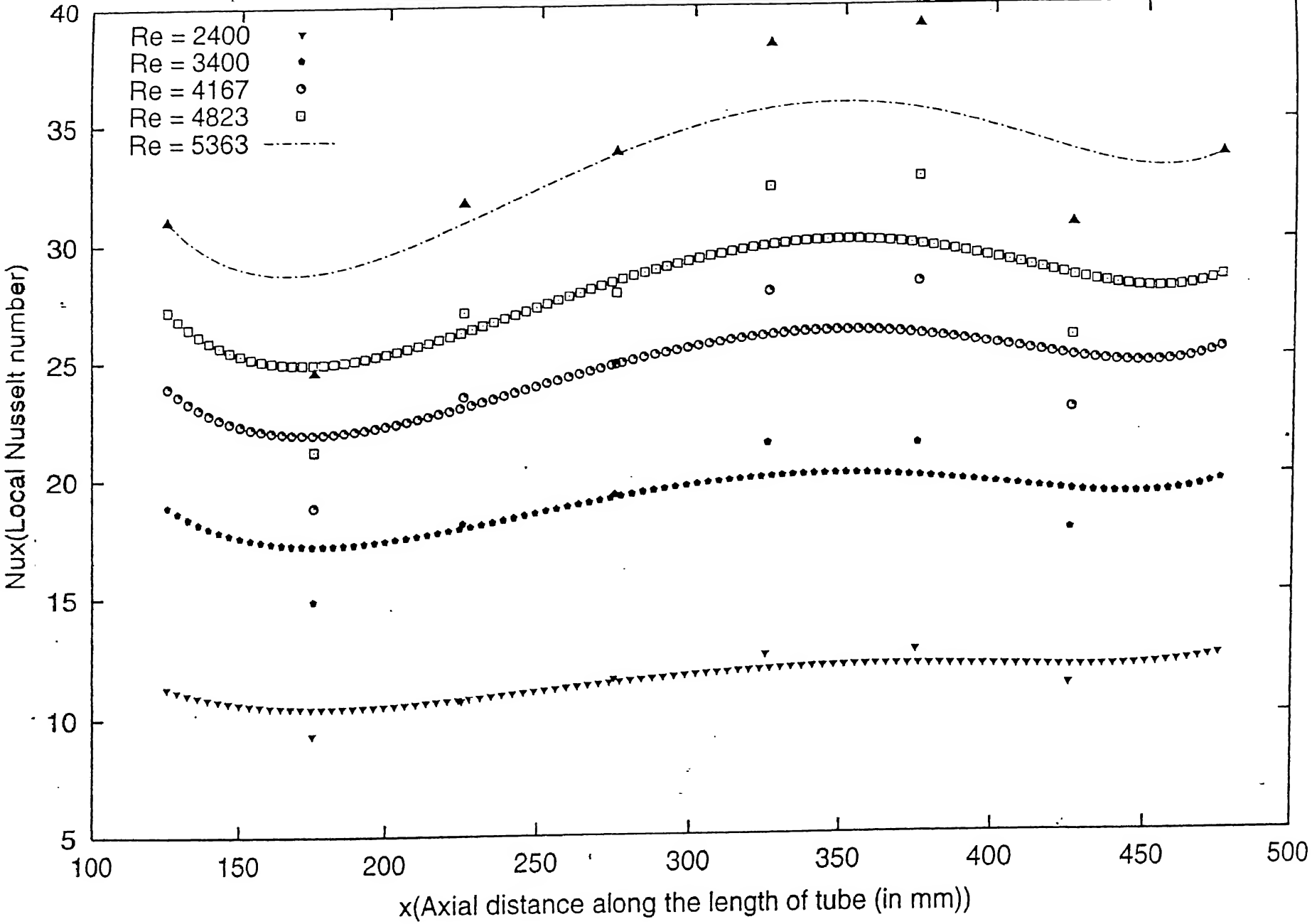

Fig 4.5:Nusselt number variation along the length of tube [with pitch of 9 mm]

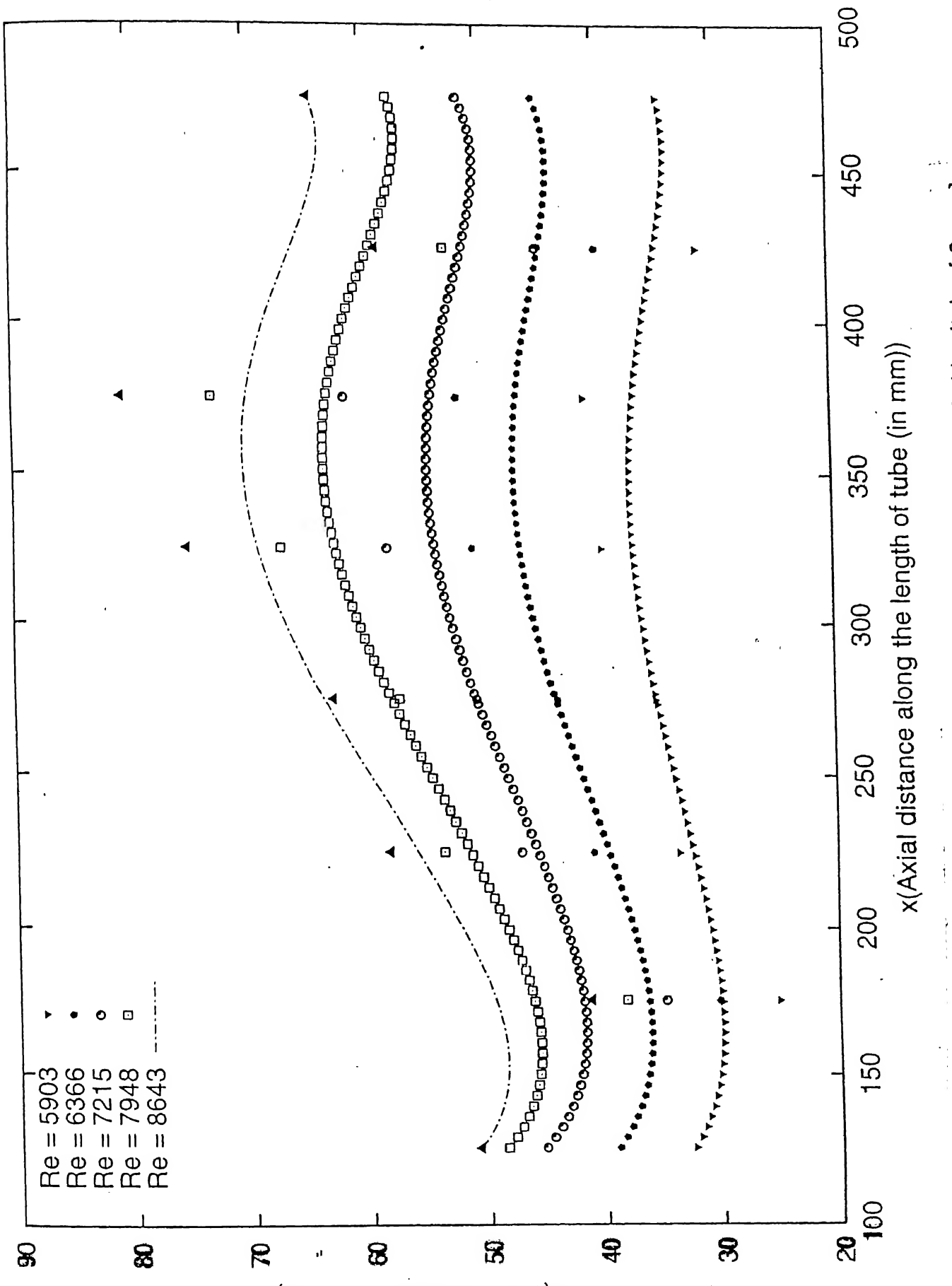
Re = 5903
Re = 6366
Re = 7215
Re = 7948
Re = 8643
Nux(Local Nusselt number)
x(Axial distance along the length of tube (in mm))
90
80
70
60
50
40
30
20
100
150
200
250
300
350
400
450
500

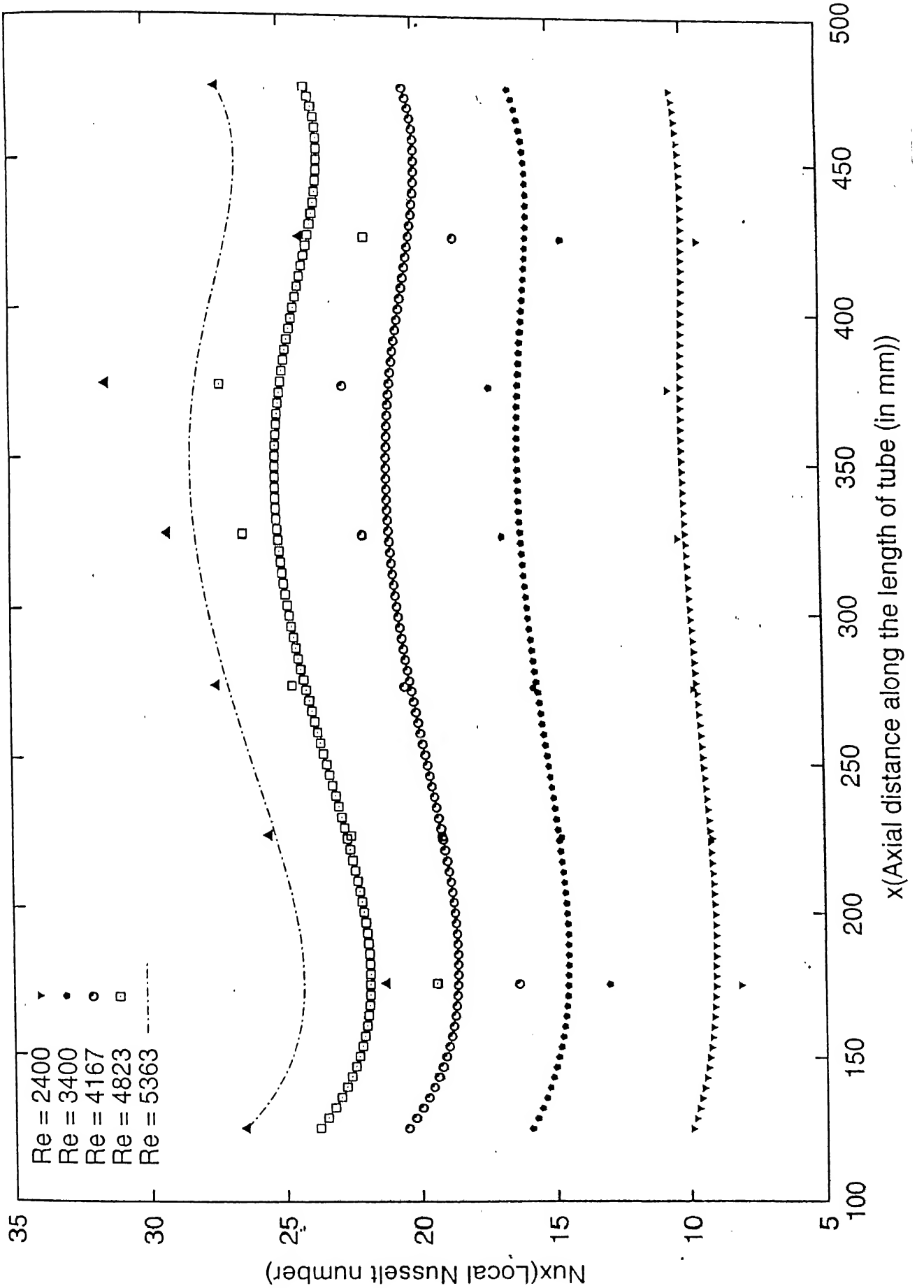
Re = 2400
Re = 3400
Re = 4167
Re = 4823
Re = 5363
Nux(Local Nusselt number)
x(Axial distance along the length of tube (in mm))
35
30
25
20
15
10
5
100
150
200
250
300
350
400
450
500

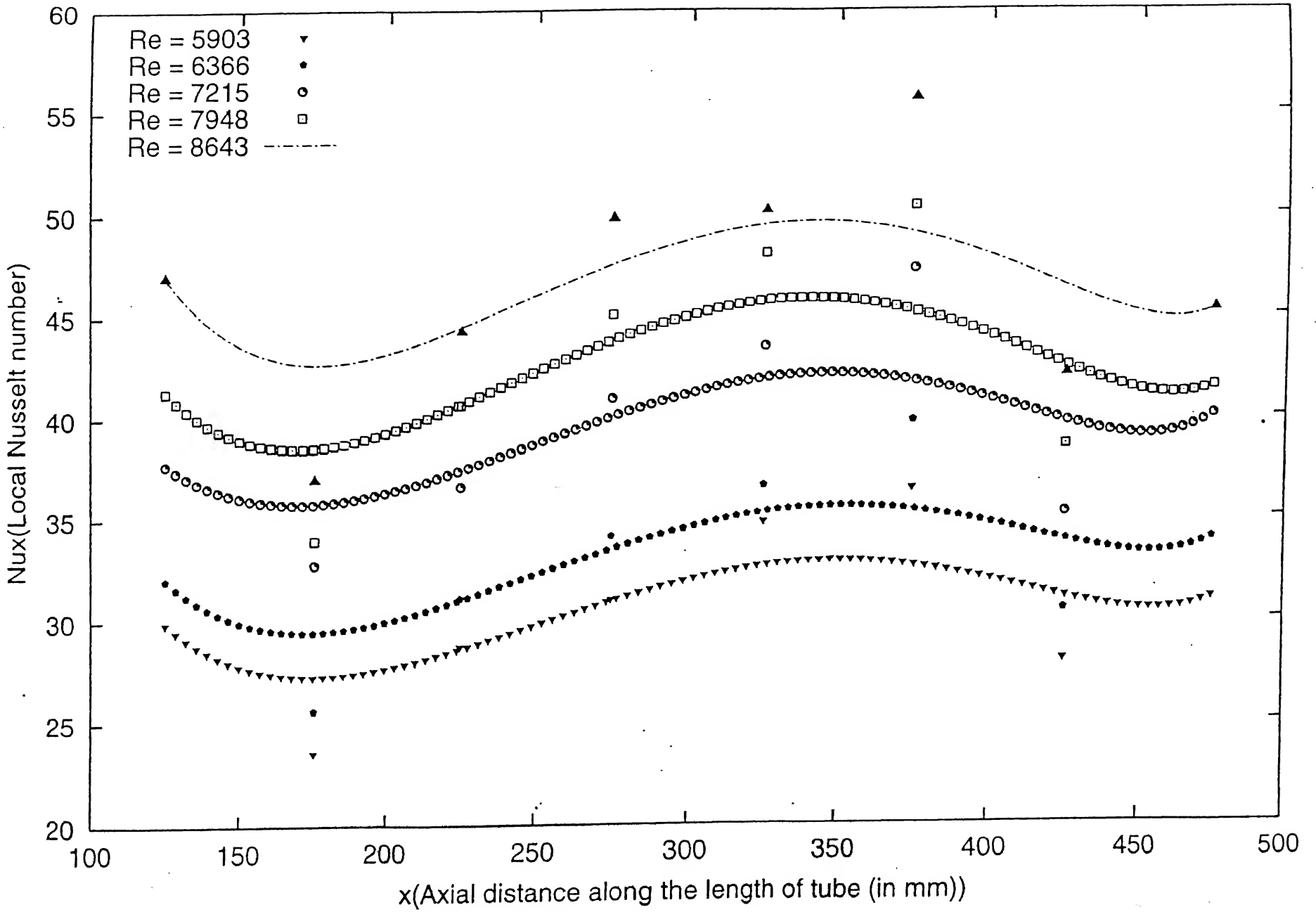
Re = 5903
Re = 6366
Re = 7215
Re = 7948
Re = 8643
Nux(Local Nusselt number)
x(Axial distance along the length of tube (in mm))
60
55
50
45
40
35
30
25
20
100
150
200
250
300
350
400
450
500

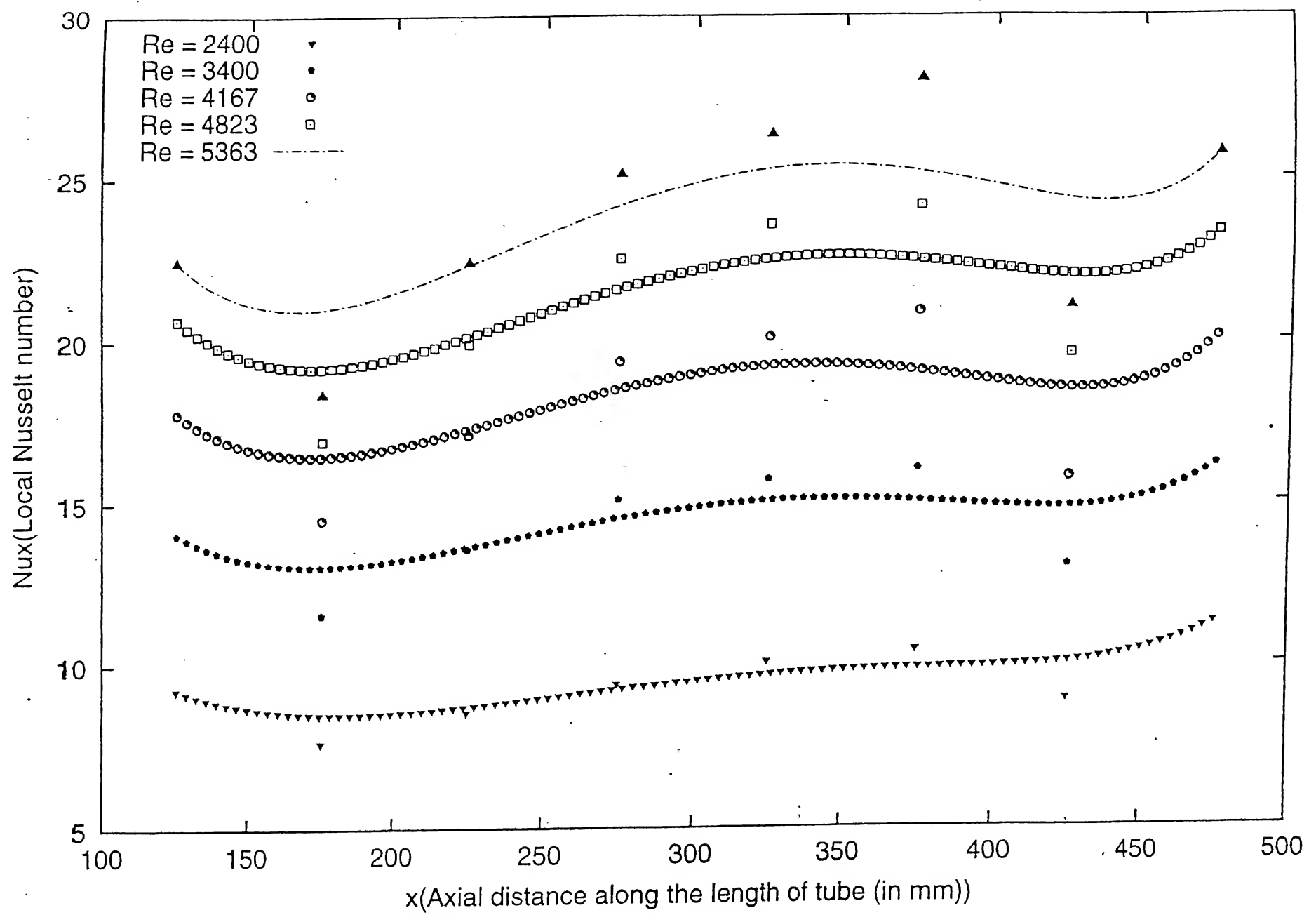
Re = 2400
Re = 3400
Re = 4167
Re = 4823
Re = 5363
Nux(Local Nusselt number)
x(Axial distance along the length of tube (in mm))
30
25
20
15
10
5
100
150
200
250
300
350
400
450
500

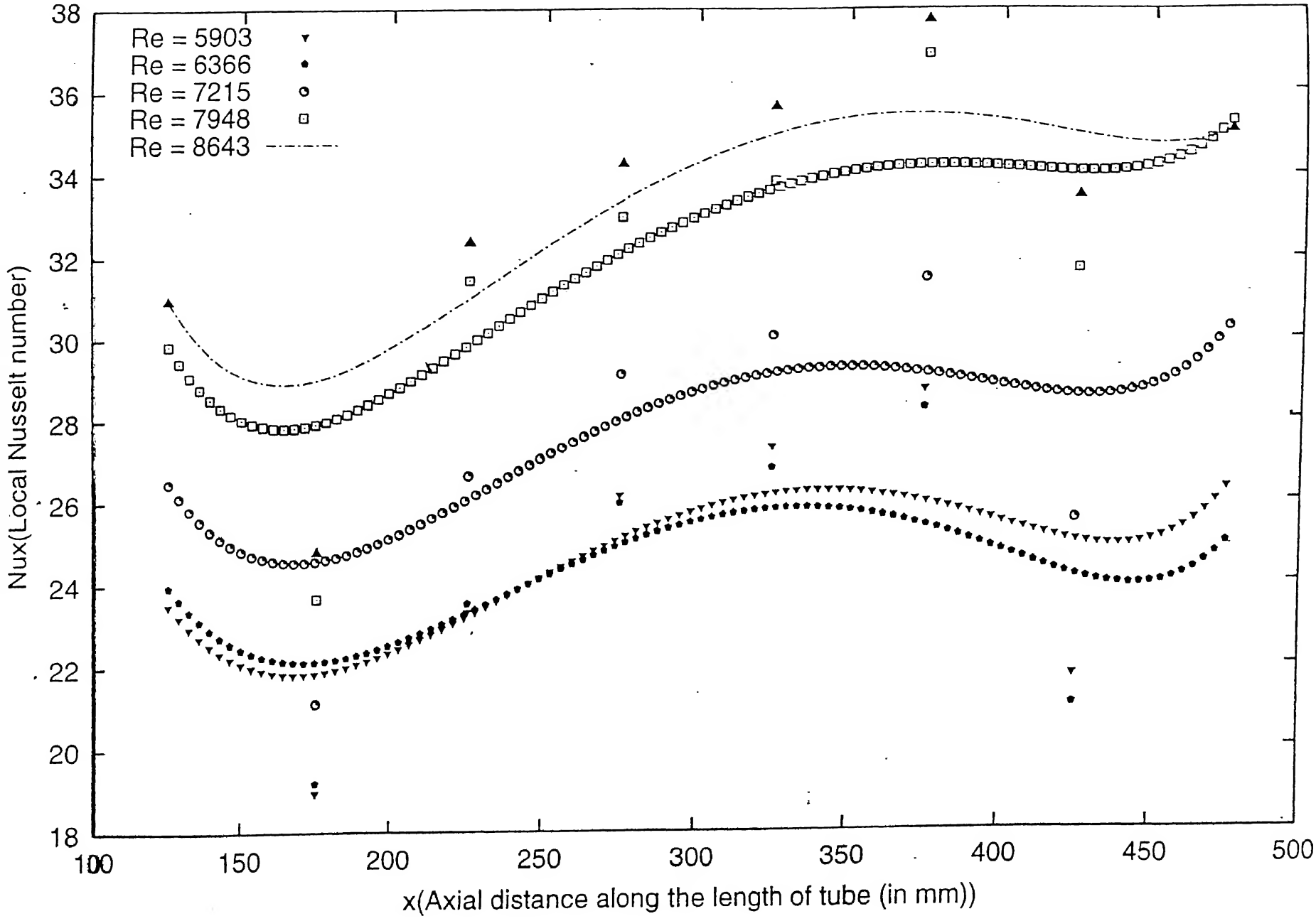
Re = 5903
Re = 6366
Re = 7215
Re = 7948
Re = 8643
Nux(Local Nusselt number)
x(Axial distance along the length of tube (in mm))
38
36
34
32
30
28
26
24
22
20
18
100
150
200
250
300
350
400
450
500

Table 4.6: Average Nusselt number variation with Reynolds number

Reynolds Number (Re)	Smooth Tube	Tube with coil springs in various pitches			
		4 mm pitch	9 mm pitch	15 mm pitch	42 mm pitch
2400	7.992	8.891	11.419	9.644	9.321
3400	11.759	13.629	18.846	15.437	14.295
4167	14.914	19.204	24.377	19.934	18.100
4823	17.950	21.835	27.825	23.705	21.247
5363	20.258	24.579	32.885	26.570	23.622
5903	22.420	28.222	34.225	30.422	24.450
6366	23.855	31.917	42.755	32.942	24.177
7215	26.534	38.598	49.473	39.309	27.474
7948	29.800	46.045	56.429	42.585	31.864
8643	30.249	51.428	62.036	46.431	33.022

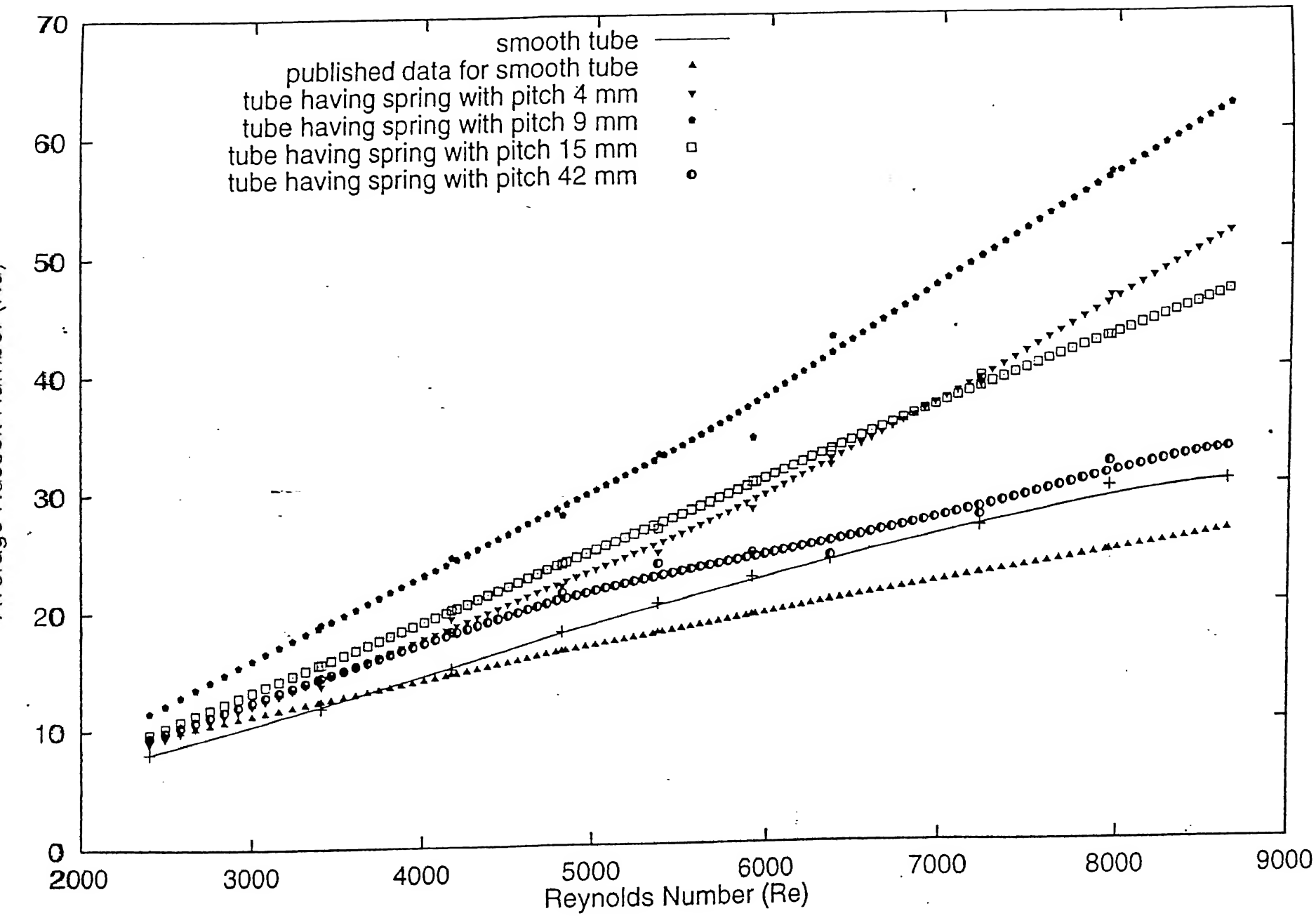
smooth tube
published data for smooth tube
tube having spring with pitch 4 mm
tube having spring with pitch 9 mm
tube having spring with pitch 15 mm
tube having spring with pitch 42 mm
70
60
50
40
30
20
10
0
2000
3000
4000
5000
6000
7000
8000
9000
Reynolds Number (Re)

Step: 1

$$Tw_{125} = \frac{74.2 + 74.0}{2} = 74.1^{o} C$$

Step: 2

$$Ta_{125} = Ta_i + \frac{Ta_o - Ta_i}{L} \times 125$$
$$= 34.7 + \frac{65 - 34.7}{600} \times 125$$
$$= 41.013^{o} C$$

Step: 3

$$\rho_a = 1.15 kgm^{-3}$$
$$\mu = 2 \times 10^{-5} kgm^{-1} s^{-1}$$

Using Eq. (4.1)

$$\dot{m} = 6.22 \times 10^{-4} kgs^{-1}$$

Step: 4

Using Eq. (4.2)

$$Re = 2399.86 \approx 2400$$

Step: 5

$$C_p = 1.007 KJ/kg^{o} C$$
$$k_b = 0.027 W/m \ K$$
$$A_S = \pi D_i L$$

using Eq.(4.5)

$$Nu_{125} = 11.27$$

4.3 Evaluation of Friction factor:

Pressure drop across the test section was been measured by an inclined tube manometer. The friction factor was calculated using following expression:

$$f = \left(\frac{\rho_L g A^2 D_i}{2L} \right) \frac{h \rho_a}{\dot{m}^2} \qquad (4.7)$$

where,

ρ_L : density of manometric fluid

A_t : cross section area of the tube

D_i : inside diameter of the tube

L : length of the tube

h : reading of inclined tube manometer

Using the above equation the friction factors were calculated and are given in Table 4.7. Their plots are shown in Fig.4.12

4.4 Comparison with Published Data (Smooth Tube)

The experiments were conducted over a Reynolds number range of approximately 2400 to 9000. The apparatus, instrumentation, and procedure were checked by comparing the experimental data on a smooth tube with those from literature.

The heat transfer data (fig-4.11) were found to be in good agreement with those obtained from the correlation for the turbulent region (Petukhov and Popov, 1963, $Nu = 0.022 \quad Pr^{0.5} \quad Re^{0.8}$).Therefore the apparatus and instrumentation were considered good enough for taking required data on the test section with springs.

Table 4.7: Fanning friction factor variation with Reynolds number

Reynolds Number (Re)	Smooth Tube ($\times 10^{-3}$)	Tube with coil springs in various pitches			
		4 mm pitch	9 mm pitch	15 mm pitch	42 mm pitch
2400	7.295	0.0620	0.1095	0.0563	0.0270
3400	7.299	0.0576	0.121	0.0631	0.0248
4167	7.315	0.0547	0.1002	0.0606	0.0256
4823	7.308	0.0487	0.0730	0.0533	0.0226
5363	5.912	0.0457	0.0683	0.0506	0.0201
5903	6.111	0.0422	0.0625	0.0471	0.0189
6366	5.805	0.0402	0.0577	0.0425	0.0176
7215	5.354	0.0358	0.0510	0.0356	0.0152
7948	5.100	0.0321	0.0479	0.0343	0.0144
8643	4.630	0.0285	0.0420	0.0320	0.0136

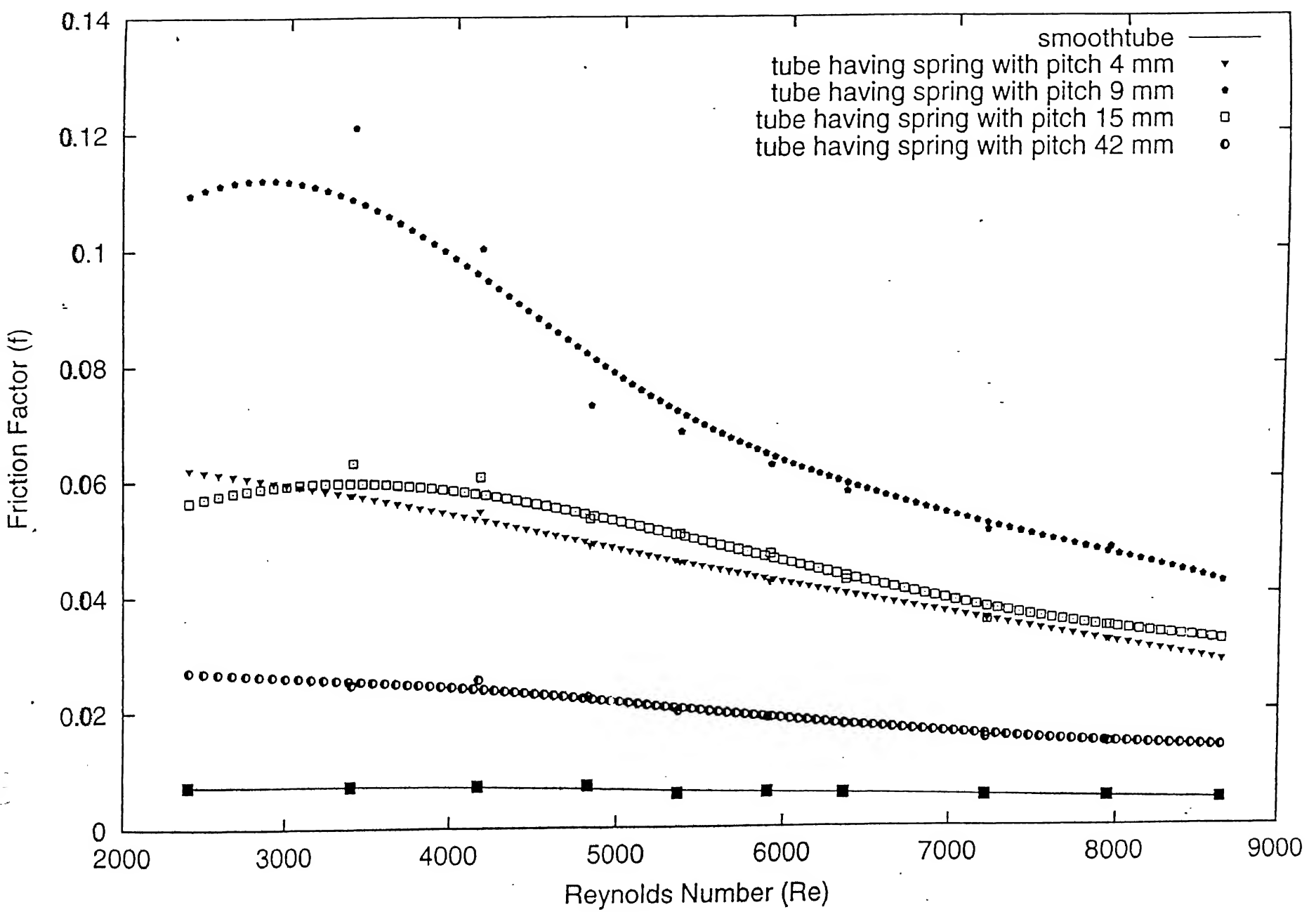
smoothtube
tube having spring with pitch 4 mm
tube having spring with pitch 9 mm
tube having spring with pitch 15 mm
tube having spring with pitch 42 mm
Friction Factor (f)
Reynolds Number (Re)
0.14
0.12
0.1
0.08
0.06
0.04
0.02
0
2000
3000
4000
5000
6000
7000
8000
9000

4.5 Analysis:

As mentioned above, to evaluate the performance of the augmenting geometry a parameter η (called efficiency index) was calculated. It is defined as:

$$\eta = \frac{Nu(et)/Nu(st)}{f(et)/f(st)} \qquad (4.8)$$

Values of η are given in Table (4.10).

4.5.1 Data Reduction:

It had been observed, after calculation, that the local Nusselt Numbers are exceptionally very high at the locations which were near to inlet and outlet of the test section. This was more in case of locations x = 525 mm and x = 575 mm which were very near to outlet of the tube. This can be explained in terms of insufficient thickness of the insulation (Gasket seals between the flanges at the outlet and inlet of the test section). Because of insufficient thickness heat loss was very large at the inlet and outlet of the tube (total heat loss varies from 22% to 62%). This resulted in lower temperature of the wall near the both ends. As a result local Nusselt Number increased to high value at these locations. Therefore these data (data at x =25 mm, x = 525 mm and x = 575 mm) did not show the true behavior of local Nusselt Number. Hence the data at these points were excluded while plotting Nu_x. Further while calculating Nu (average Nusselt Number) they were not taken into account.

4.5.2 Analysis of various parameters :

Fig. 4.1 to Fig. 4.10 show the variation of Local Nusselt Number, Nu_x, with the axial distance for various values of Reynolds Number ,Re. It is observed that :

- As Re increases, Nu_x increases. This is because at higher Reynolds Number turbulence increased which resulted in better flow mixing and consequently better heat transfer.

Table 4.8: Variation of fractional increase in Nusselt number with Reynolds number

Reynolds Number (Re)	Tube with coil springs in various pitches			
	4 mm pitch	9 mm pitch	15 mm pitch	42 mm pitch
2400	1.112	1.429	1.207	1.166
3400	1.159	1.603	1.313	1.216
4167	1.288	1.635	1.337	1.214
4823	1.216	1.550	1.321	1.184
5363	1.213	1.623	1.312	1.166
5903	1.259	1.527	1.357	1.091
6366	1.338	1.792	1.381	1.013
7215	1.455	1.865	1.481	1.035
7948	1.545	1.894	1.429	1.069
8643	1.700	2.051	1.535	1.092

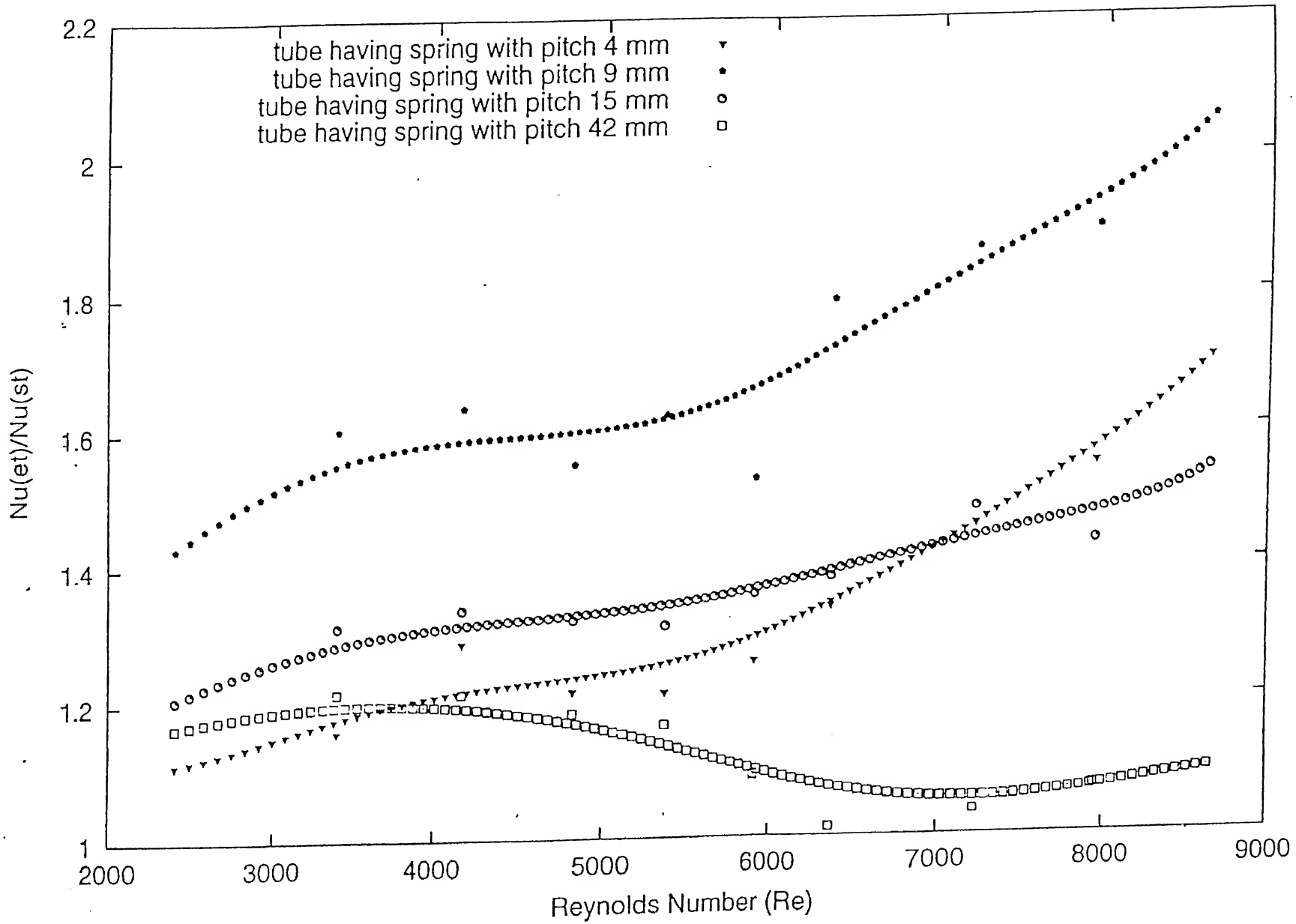

Fig. 4.10:Variation of fractional increase in Nusselt Number with Reynolds Number

Table 4.9: Variation of fractional increase in fanning friction factor with Reynolds number

Reynolds Number (Re)	Tube with coil springs in various pitches			
	4 mm pitch	9 mm pitch	15 mm pitch	42 mm pitch
2400	8.499	15.010	7.718	3.701
3400	7.891	16.978	8.645	3.398
4167	7.666	14.043	8.493	3.588
4823	6.664	9.989	7.293	3.093
5363	7.730	11.553	8.559	3.400
5903	6.906	10.227	7.707	3.093
6366	6.925	9.440	7.321	3.032
7215	6.687	9.526	6.649	2.839
7948	6.294	9.392	6.765	2.824
8643	6.156	9.071	6.911	2.937

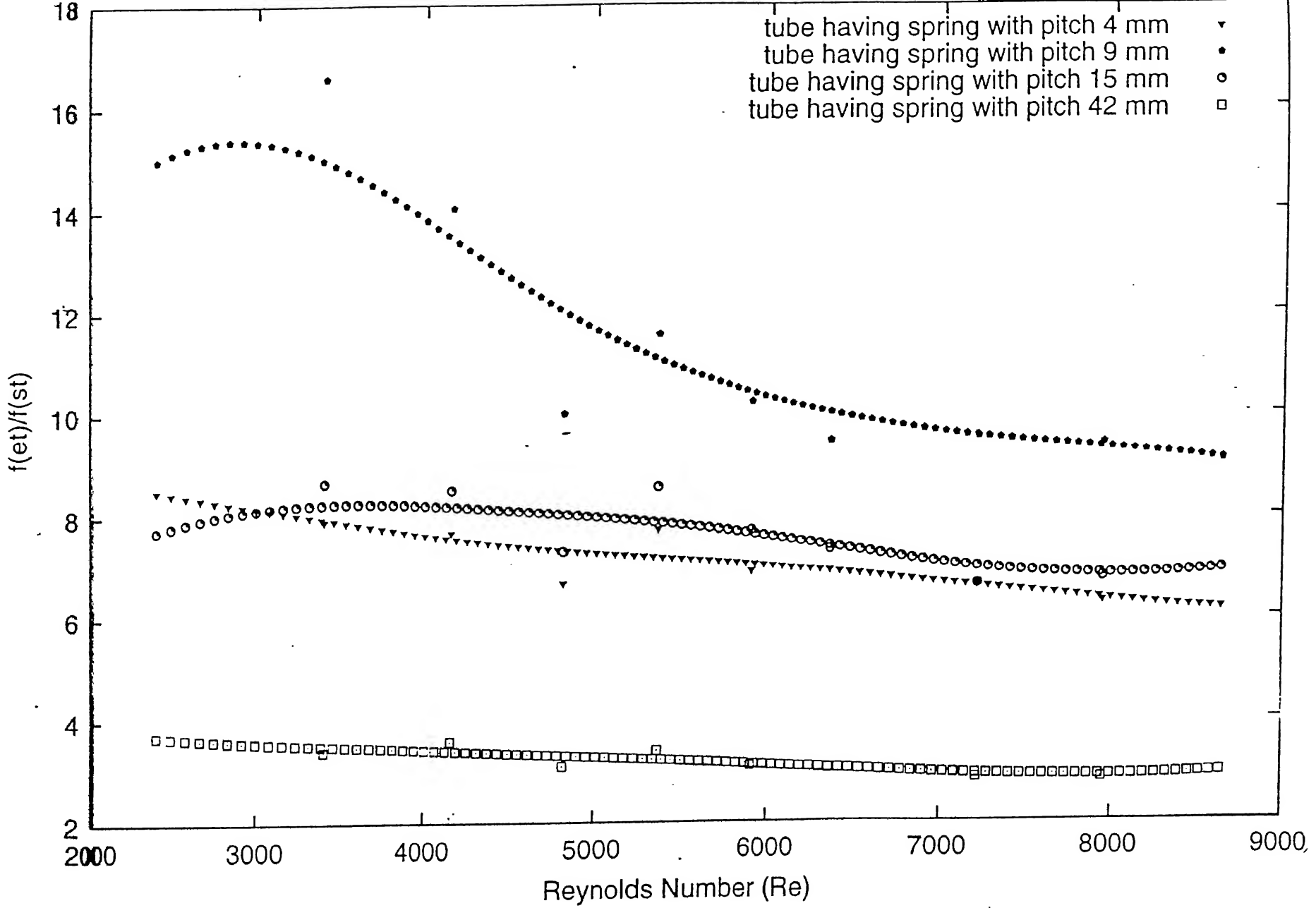

Fig 4.14:Variation of [illegible] friction factor with Reynolds Number

Table 4.10: Variation of efficiency index with Reynolds number

Reynolds Number (Re)	Tube with coil springs in various pitches			
	4 mm pitch	9 mm pitch	15 mm pitch	42 mm pitch
2400	0.131	0.095	0.156	0.315
3400	0.147	0.097	0.152	0.357
4167	0.168	0.116	0.157	0.338
4823	0.182	0.155	0.180	0.383
5363	0.157	0.140	0.153	0.343
5903	0.182	0.150	0.176	0.353
6366	0.193	0.180	0.189	0.334
7215	0.217	0.196	0.222	0.365
7948	0.245	0.202	0.211	0.379
8643	0.276	0.226	0.222	0.372

- Along the axial length from inlet to outlet, generally a slight increase in N_{ux} has been seen. As we know in case of fully developed turbulent flow through a tube, subjected to a constant heat flux, • T(=Tw_x-Ta_x) remains constant along the length of tube. So the local Nusselt Number should be same along the entire length of tube. The deviation of nature of Nu_x in the experiment from the theoretical nature may be explained in two ways •

  (i) Despite the best effort to ensure uniform winding of heating tape along the length, it is possible that the heating was not uniform throughout the length.

  (ii) Thickness of the insulation (glass wool) may not be even throughout the length. This will result in heat loss to the ambient by conduction in radial direction.

Fig 4.11 shows the variation of Average Nu for smooth tube and for enhanced tubes with respect to Reynolds number. It is evident from the plot that:

- As the Reynolds number is increased, the average Nusselt number increases steadily for all types of tubes .i.e. smooth tubes and enhanced tubes. Overall it is evident that as the flow becomes more turbulent, the average Nusselt number keeps on increasing.

Fig 4.12 shows the variation of fanning friction factor with Reynolds number. It is observed that,

- Friction factor for smooth tube decreases very slowly in turbulent region as we increase the turbulence by increasing the Re. These experimental data showed the expected trend.
- The value of friction factor for the enhanced tube, f increases to a maximum(this is more prominent in case of tubes having springs of pitch 9 mm and 15 mm) and then starts decreasing and then tends to become a constant.
- In general the friction factor for enhanced tubes having springs of different pitches is more than that for the smooth tube. This is expected because by

inserting a spring in the tube, turbulence was increased, therefore the resistance to flow was also increased.

Fig. 4.13 shows the variation of fractional increase of Nu, [Nu(et)/Nu(st)], with Re. It can be seen that,

- For the tubes having springs of 4, 9, 15 mm pitches the ratio Nu(et)/Nu(st) increases in general. However, for tube with of 42 mm pitch it remains more or less constant and slightly greater than one. This may be because, as we increase the pitch of spring, the enhanced tube starts behaving more and more like a smooth tube.

Fig 4.14 shows the variation of fractional increase in friction factor,[f(et)/f(st)], with Re for enhanced tubes. It is seen that,

- In general this ratio decreases slowly as Re is increased. The ratio is minimum for the tube having spring of 42 mm pitch and maximum for the tube having spring of 9 mm pitch.

Fig. 4.15 shows the variation of efficiency index, η, with Re and it is seen that,

- As Re increases, efficiency increases. However, the rates of increase are different with different springs.
- It is maximum for tube having spring with a pitch of 42 mm. It is because, though the heat transfer augmentation is small, but simultaneously the increase in pressure drop is so small, that the efficiency ,η , becomes high.

Figures 4.16 to 4.23 show the variation of Average Nusselt number (4.16, 4.17), friction factor(4.18, 4.19), Nu(et)/Nu(st) (4.20, 4.21) and f(et)/f(st) (4.22, 4.23) with pitch of the spring, used in the tube as an augmenting device. It is seen,

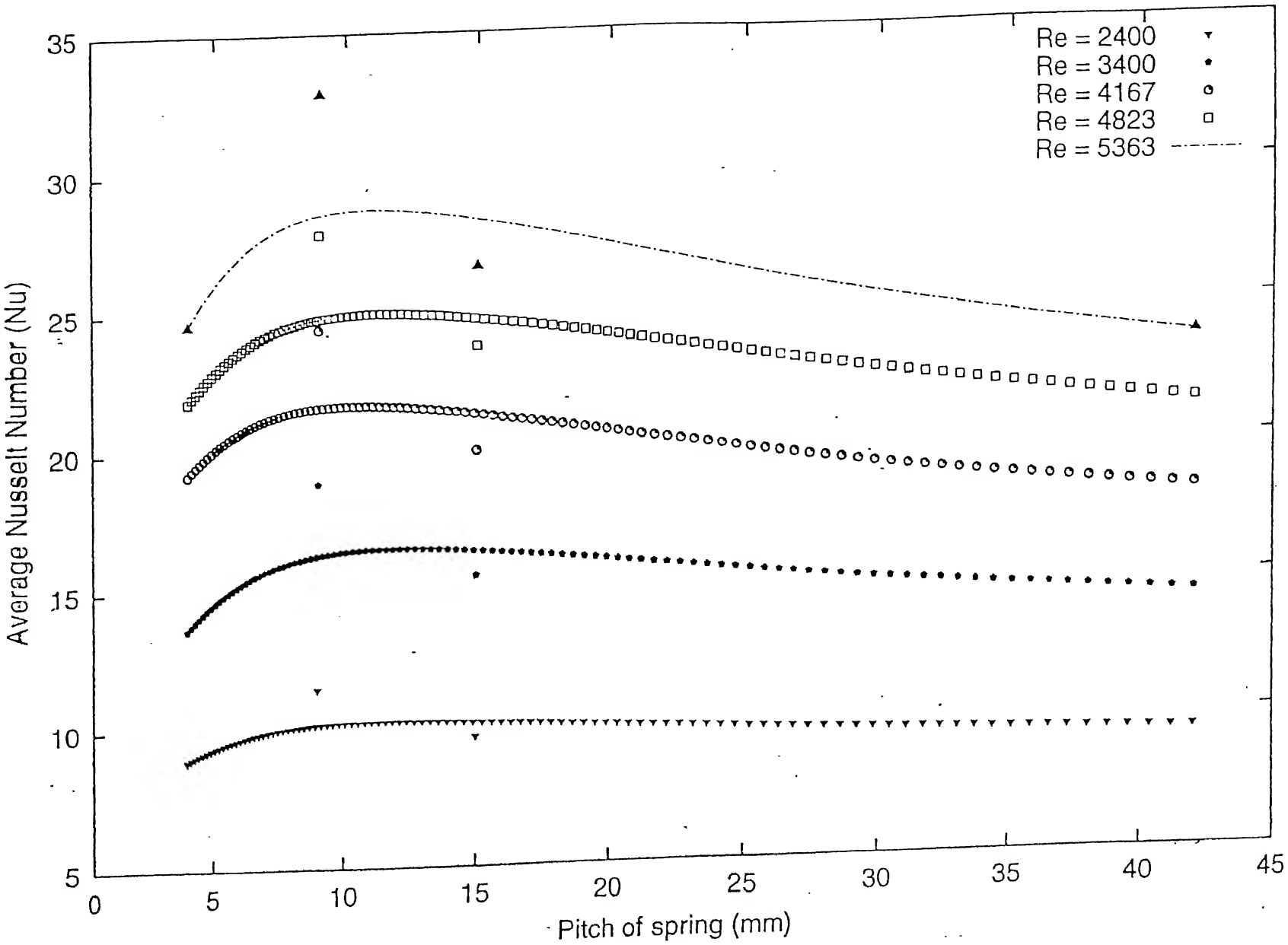

Fig 4.16:Variation of Nusselt Number with pitch of the spring

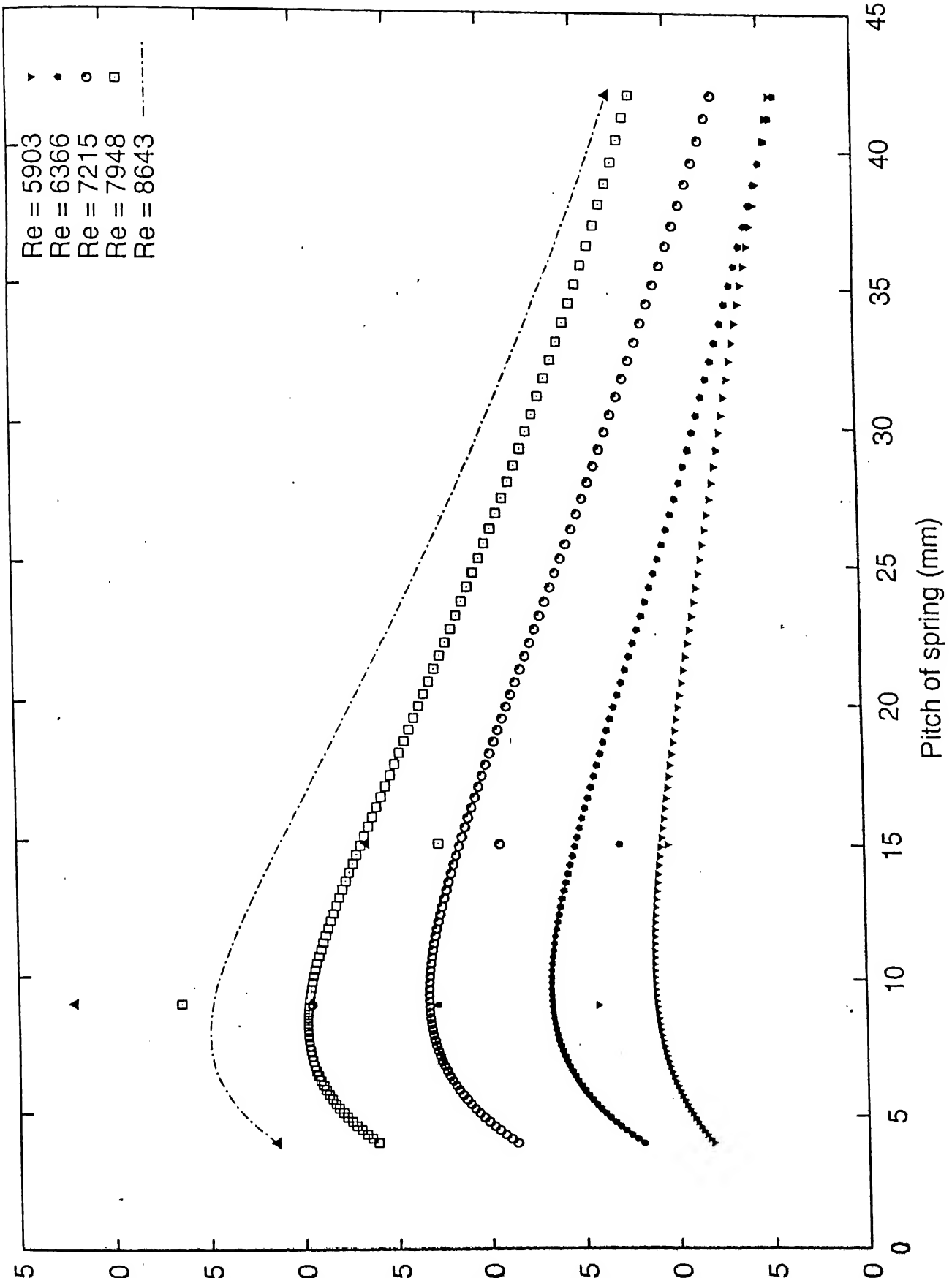
Re = 5903
Re = 6366
Re = 7215
Re = 7948
Re = 8643
Average Nusselt Number (Nu)
Pitch of spring (mm)
65
60
55
50
45
40
35
30
25
20
0
5
10
15
20
25
30
35
40
45

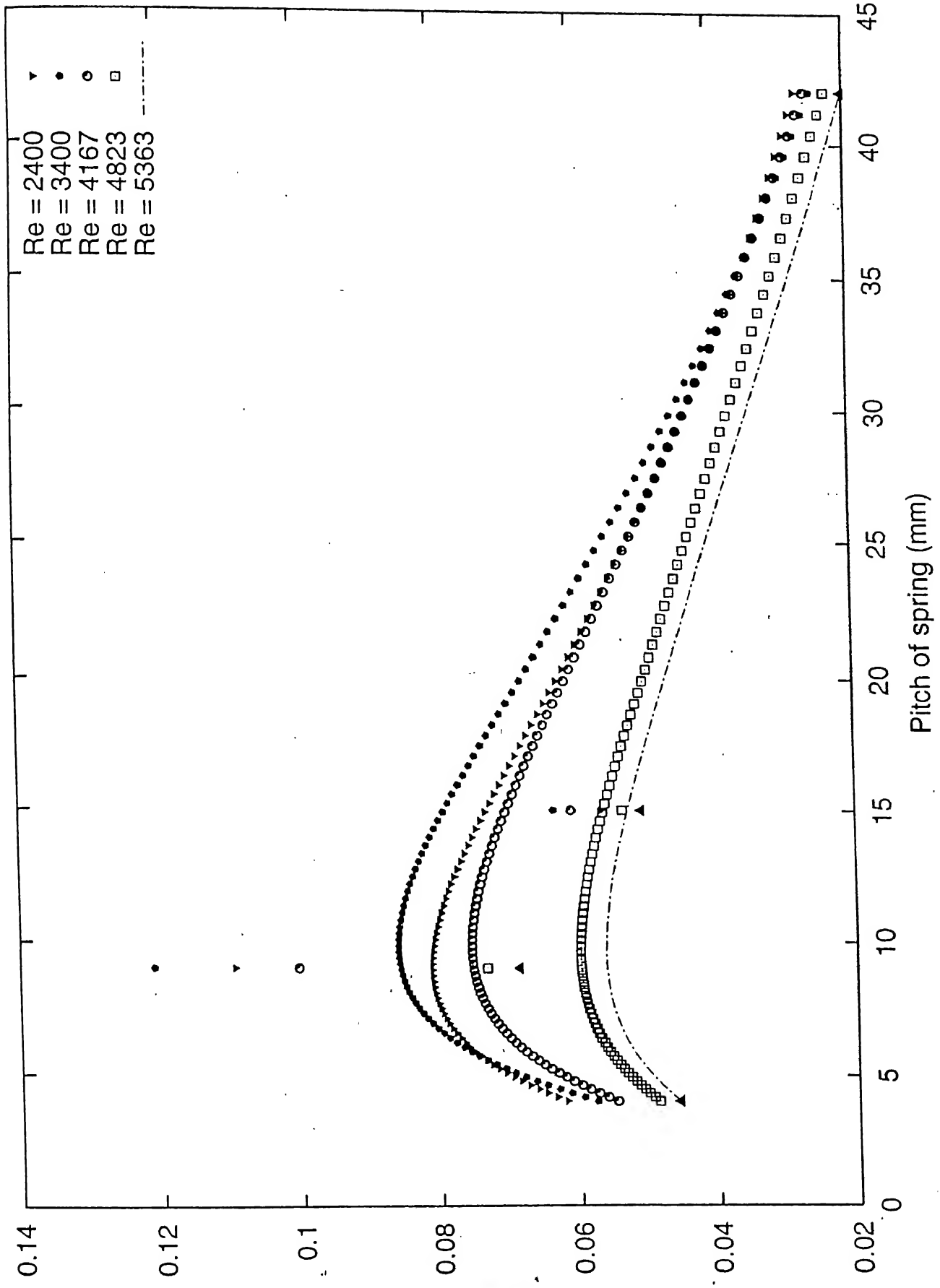
Re = 2400
Re = 3400
Re = 4167
Re = 4823
Re = 5363
0.14
0.12
0.1
0.08
0.06
0.04
0.02
0
5
10
15
20
25
30
35
40
45
Pitch of spring (mm)

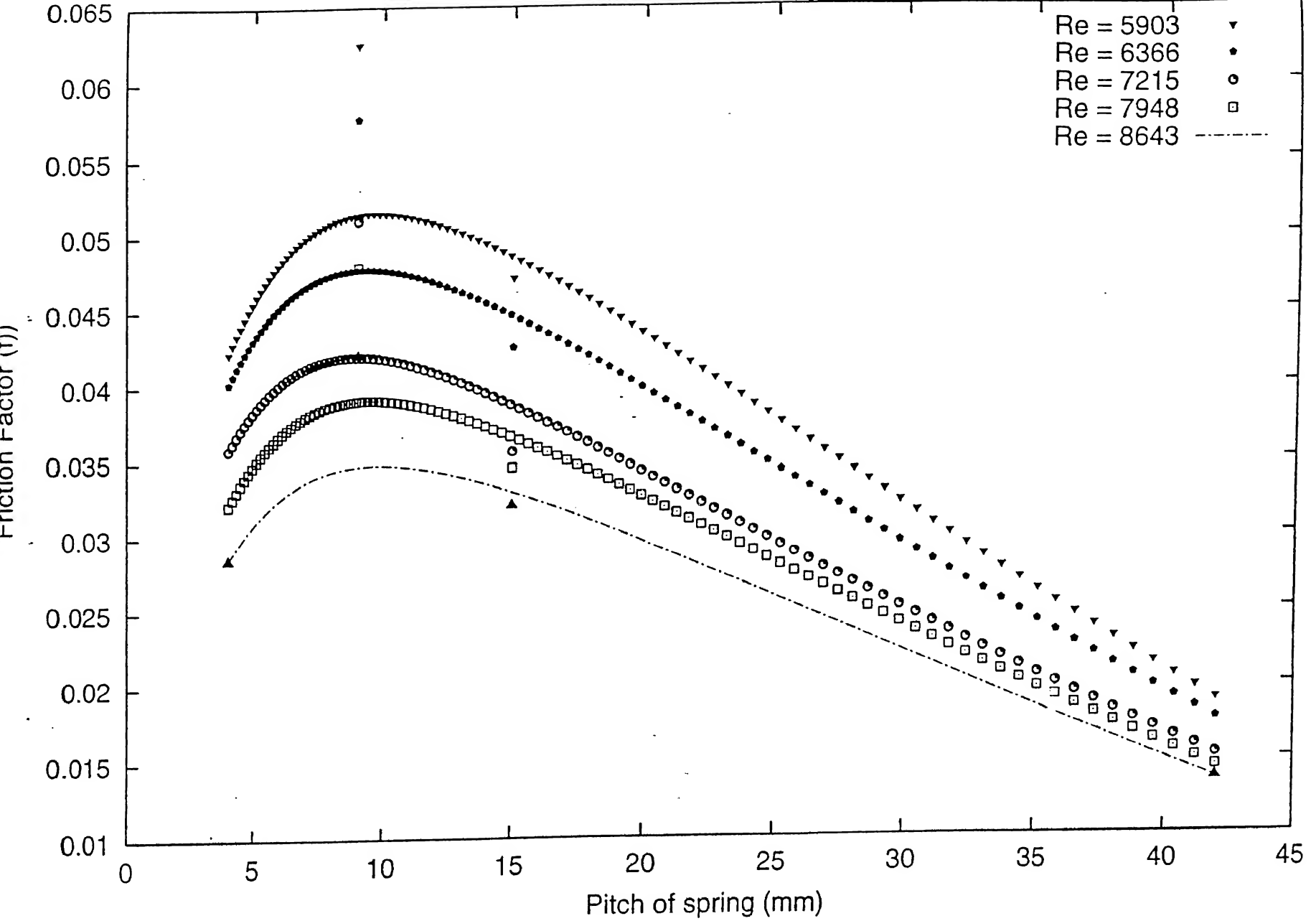

Fig 4.19:Variation of Friction Factor with pitch of the spring

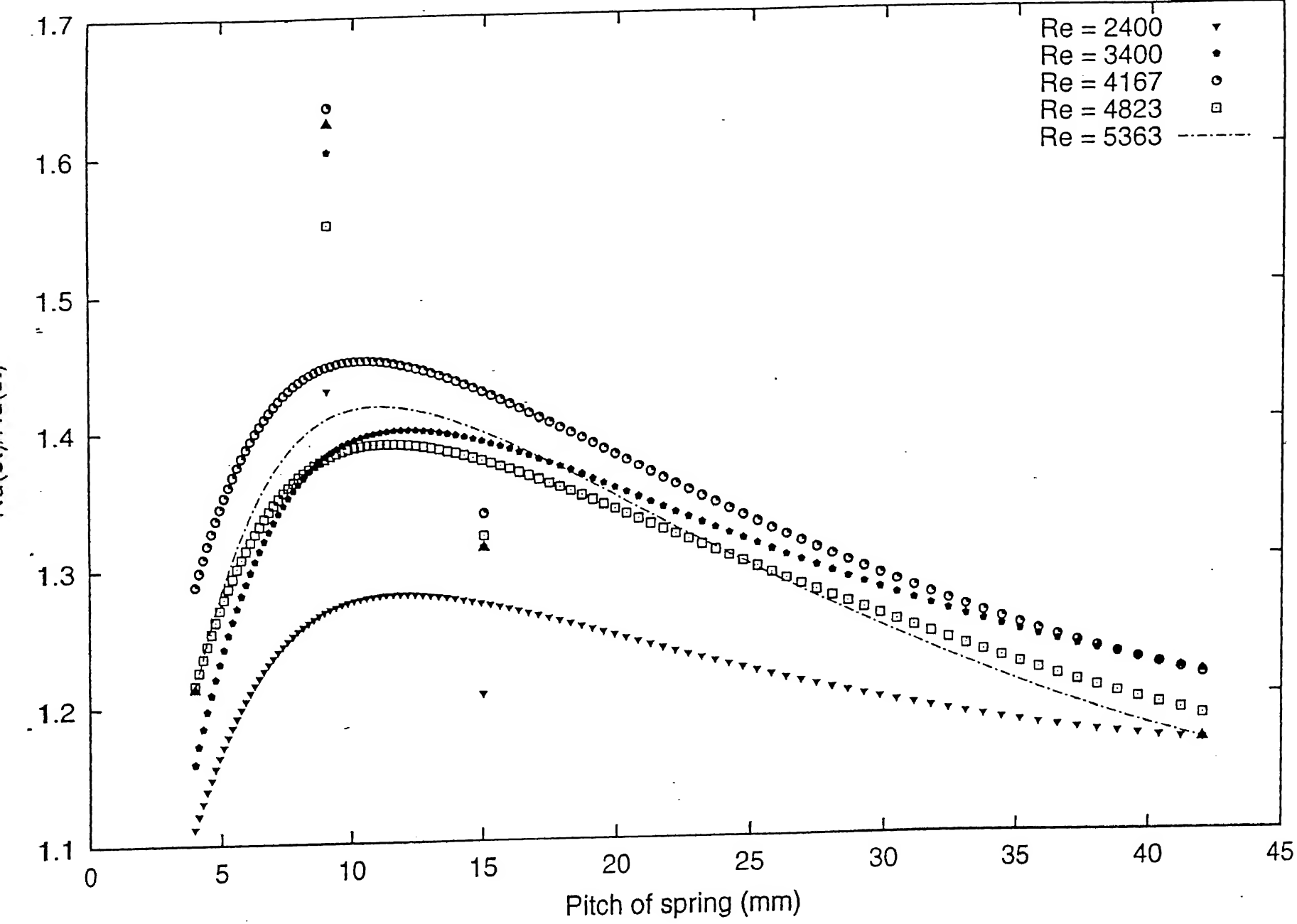

Fig 4.20:Variation of Fractional increase of Nusselt Number with pitch of the spring

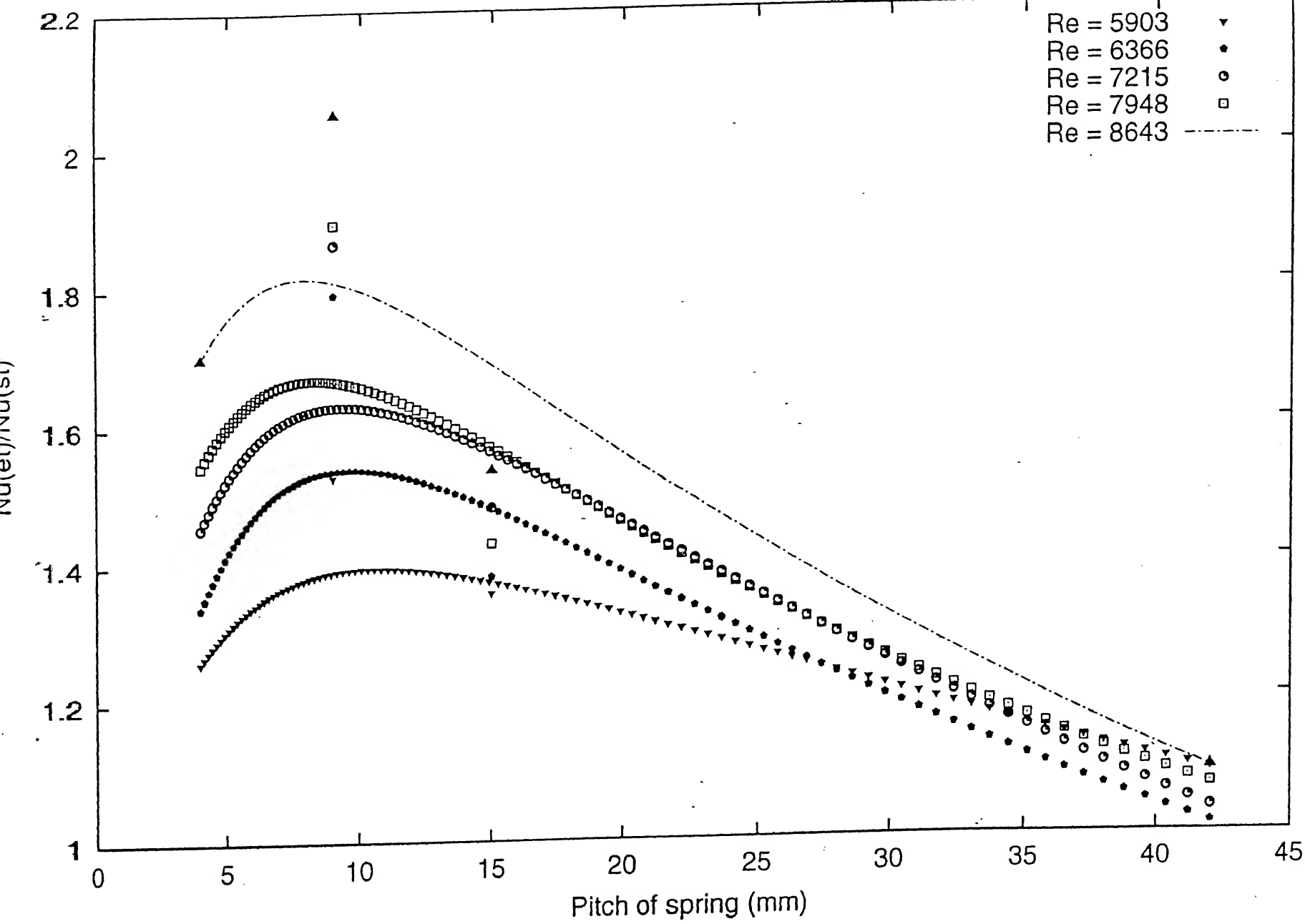

Fig 4.21 Variation of Fractional increase of Nusselt Number with pitch of the spring

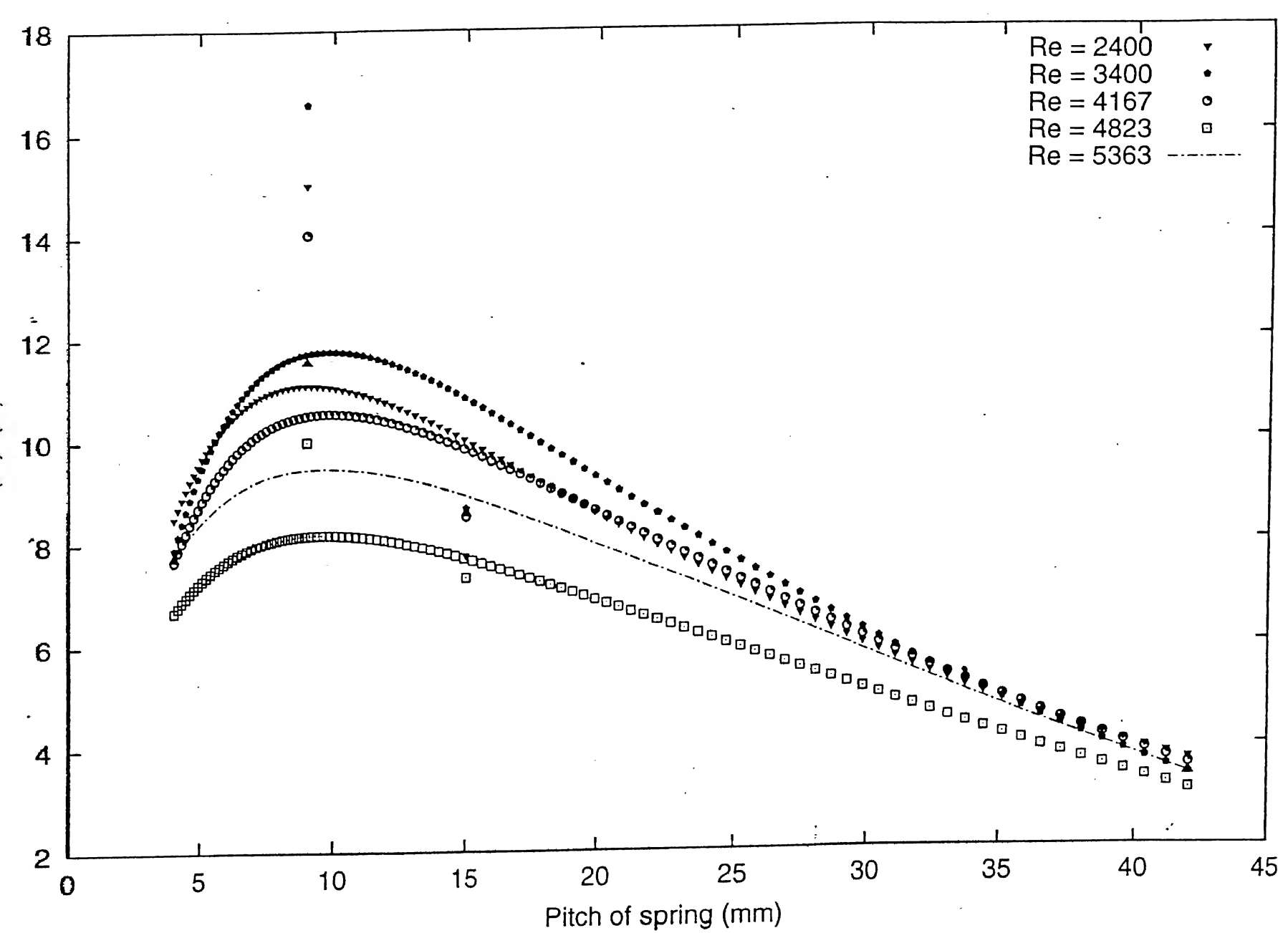
Re = 2400
Re = 3400
Re = 4167
Re = 4823
Re = 5363
18
16
14
12
10
8
6
4
2
0
5
10
15
20
25
30
35
40
45
Pitch of spring (mm)

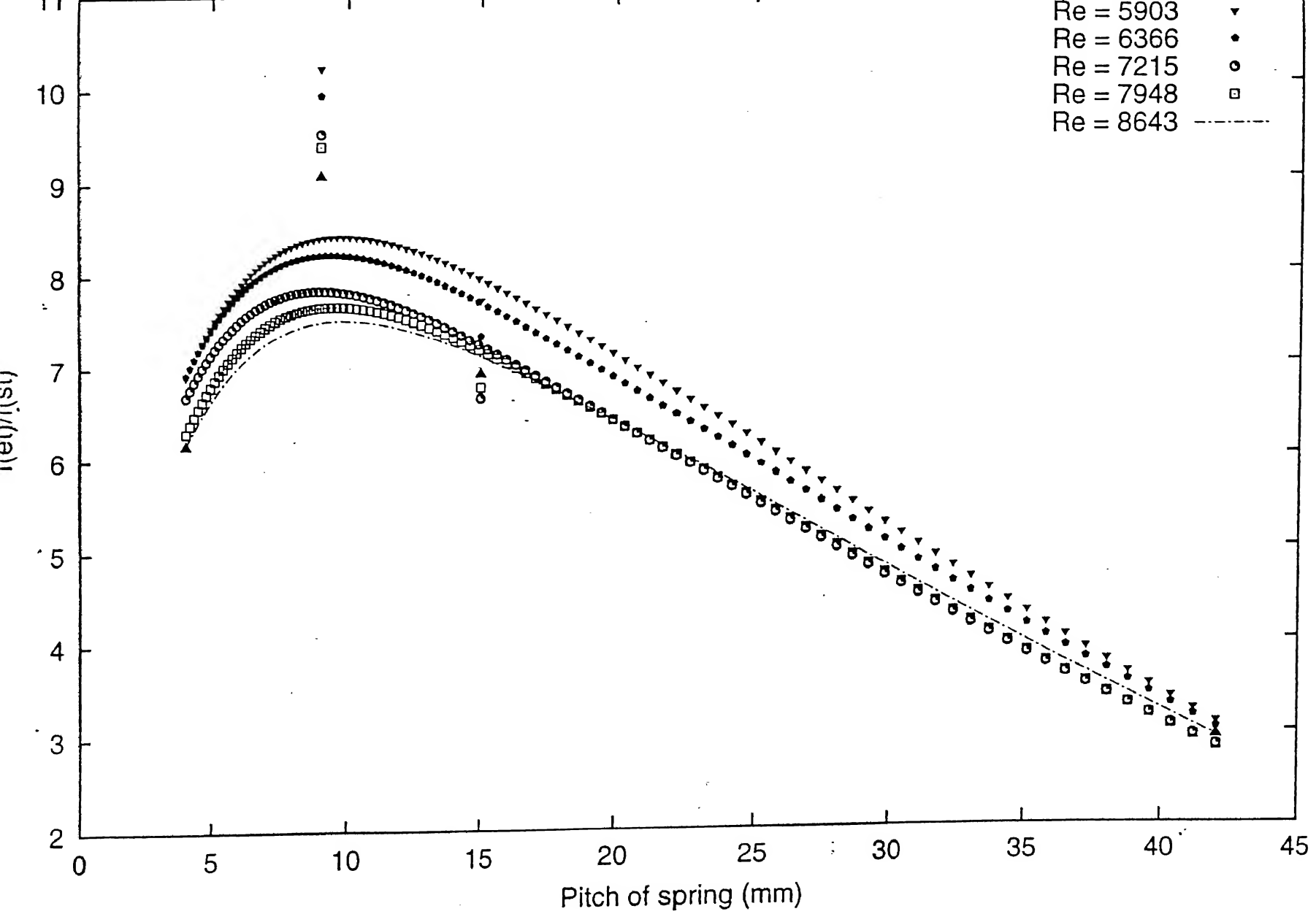

Fig 4.23:Variation of Fractional increase of Friction Factor with pitch of the spring

- In all the plots as we increase the pitch of spring the Nu, f, Nu(et)/Nu(st) and f(et)/f(st) first increase, reach a maximum and then start decreasing. The probable explanation is as follows,

  When the pitch of spring is very small the tube with spring behaves more like a smooth tube of reduced diameter. Therefore, as in smooth tube, the augmentation of heat transfer and increase in pressure drop are less. As we increase the pitch of spring the resistance to flow starts increasing. The flow gets disturbed and looses its characteristic of fully developed flow. As a result turbulence increases and heat transfer and pressure drop increase. However as the pitch of spring becomes very large the flow behaviour again started tending to be more like the smooth tube of original diameter. Therefore, again heat transfer and pressure drop across the section decrease. That is why we find a maxima in all these plots.

Fig 4.24 • Fig 4.25 shows the variation of efficiency index with pitch of the spring. It is clear that,

- The efficiency index plots have a minima in between 5 and 10 mm pitch. Although the heat transfer augmentation is largest for the spring with pitch of 9 mm, the increase in pressure drop is so large that the efficiency index is minimum.
- On the other hand the efficiency for 42 mm pitch spring is higher. It is because the increase in pressure drop is very less vis a vis increase in heat transfer.

4.6 CONCLUSIONS

Experimental studies on fully developed flow through a tube subjected to a constant heat flux and with helical coil springs as the heat transfer augmenting device placed in the flow demonstrated the following:

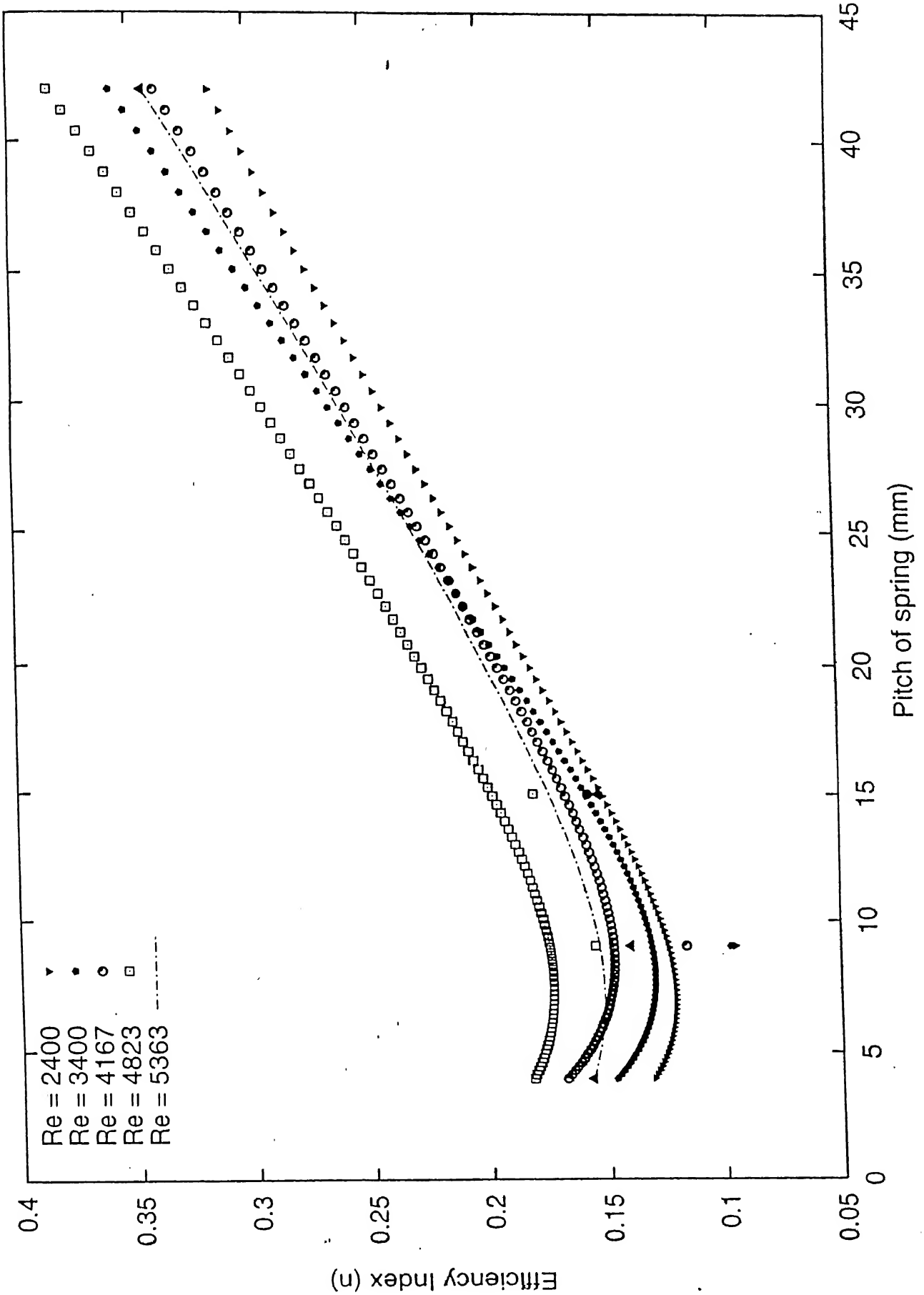
Re = 2400
Re = 3400
Re = 4167
Re = 4823
Re = 5363
Efficiency Index (n)
Pitch of spring (mm)
0.4
0.35
0.3
0.25
0.2
0.15
0.1
0.05
0
5
10
15
20
25
30
35
40
45

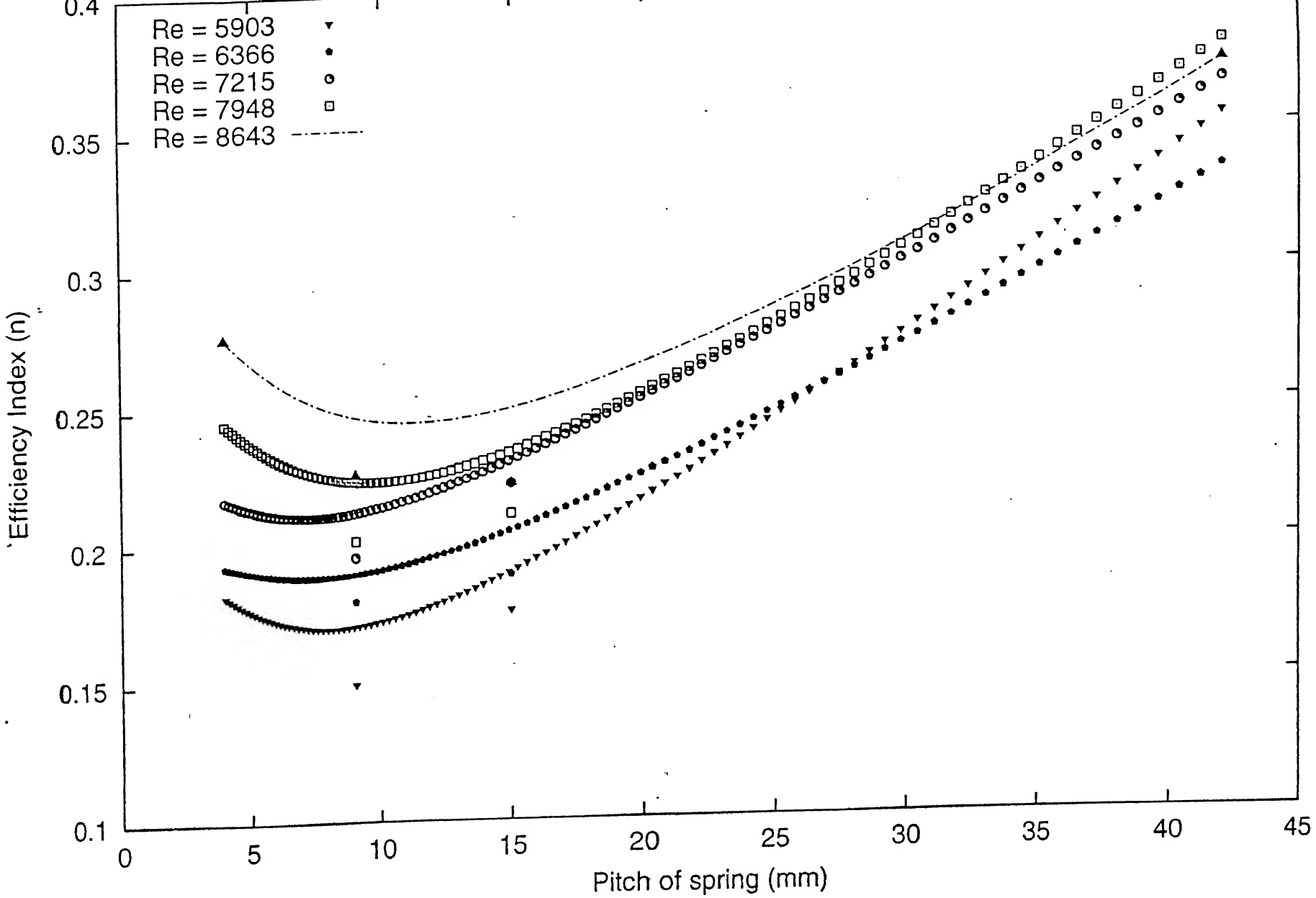
Re = 5903
Re = 6366
Re = 7215
Re = 7948
Re = 8643
Efficiency Index (n)
Pitch of spring (mm)
0.4
0.35
0.3
0.25
0.2
0.15
0.1
0
5
10
15
20
25
30
35
40
45

- The heat transfer augmentation and the increase in pressure drop is dependent not only on Re, but also on pitch of the spring. It is evident from the data that there will be one optimum pitch at which heat transfer would be maximum and so was the case with pressure drop.

- As far as the performance of this as an augmenting device was concerned, this was definitely not the best choice. It is because of the excessive pressure drop across the tube. If the spring of optimum pitch is inserted inside the tube, the heat transfer will be very large, but the corresponding pressure drop is so large that the pumping power for fluid flow will increase to very large extent and will be undesirable.

- If we compare this device with the other devices mentioned in Table 2.1, it is definitely better than the mesh inserts, brush inserts and disks and rings or streamline shapes and propeller type baffles. Only the twisted tapes, wire coils and inline propellers give better performance.

However further experiments are required before assessing its performance with respect to other devices.

As described earlier, to evaluate the performance of an augmenting device efficiency index was calculated and compared with those of other devices. In the present study, efficiency index for the spring of 42 mm pitch was the highest of all the four springs. Therefore this spring should be the most suitable one of all the four springs as an augmenting device. However if we look Table 4.8, we observe that the heat transfer augmentation is lowest for this spring. This is somewhat confusing that the spring having lowest heat transfer augmentation has been judged as the most suitable augmenting device. In fact the definition of efficiency index itself is somewhat deceptive. It is unity for a smooth tube where no heat transfer augmentation takes place while it is less than unity for many devices though they are increasing the heat

transfer. Therefore we conclude that, to evaluate the performance or assess any augmenting device, efficiency index should not be used blindly.

- Efficiency index can be considered as a suitable criterion for evaluating the performance of device if the cost involved in pumping the fluid is very important. Higher the value of efficiency index, better will be the augmenting device.
- Fractional increase in Nusselt number [Nu (ET) / Nu (ST)] should be used as an evaluation criterion and not the efficiency if heat transfer is very important and not the pressure drop. Higher the fraction, better will be the augmenting device.

4.7 Suggestions for further work

As already mentioned that to predict accurately the performance of spring as an augmenting device, further experiments are required. Therefore it is suggested that,

- Experimental study with more springs with varying pitches is needed to be carried out.
- Experiments with springs made of wires of different diameter should be conducted to investigate the effect of wire diameter on heat transfer augmentation.
- Experimental study should be conducted with different types of test fluids so as to find out the effect of Prandtl number on heat transfer augmentation.
- The Re number range in the present experiment comes within the transition zone. Therefore, it is suggested that the study must be carried out at higher Reynolds number which lie in turbulent zone.

References

(1) Agarwal, S.K. and Rao, M.R., 1996, "*Heat transfer augmentation for the flow of a viscous liquid in circular tube using twisted tape inserts*", Int. J. Heat & Mass Transfer, Vol. 39, No. 17, pp. 3547-3557.

(2) Bergles, A.E., Nirmalan, V., Junkhan, G.H. 1983, "*Bibliography on augmentation of convective heat and mass transfer II*", Heat Transfer Laboratory Report HTL-31, ISU-ERI-Ames-84221, Iowa State University, December.

(3) Bergles, A.E. Jensen, M.K., Somerscales, E.F.C., and Manglik, R.M., 1991, "*Literature review of heat transfer enhancement Technology for heat exchangers in gas fired applications*", GRI Report GRI 91-0146, Gas Research Institute Chicago, IL.

(4) Chaturvedi and Kant, K., 1992, "*Heat transfer via turbulence promotion*", J. of Energy Heat and Mass Transfer.

(5) Cheng et al., 1944, "*Spirally fluted tubing prediction and measurement*" , "Proceedings of heat transfer conference" , Vol. 6 , pp 13-18

(6) Date, A.W., 1974, "*Prediction of fully developed flow in tube containing a twisted tape*", Int. J. Heat & Mass Transfer, Vol. 17, pp 845.

(7) Gupta, N. and Date, A.W., 1989, "*Friction and heat transfer characteristics of helical turbulent air flow in annuli*", J. of Heat Transfer, Vol. 111, pp 337-344.

(8) Jensen, M.K. and Vlakancic, A., 1999, "*Experimental investigation of turbulent heat transfer and fluid flow in internally finned tubes*", Int. J. Heat & Mass Transfer, Vol. 43, pp 1343-1351.

(9) Khanna, S.K. and Keshav, K., 1994, "*Forced convection heat transfer and pressure drop for air flow through an enhanced tube*", Proc. Of the first ISHMT-ASME and twelfth national heat and mass transfer conference, Jan 5-7 held at BARC Bombay, India, and pp 231-235.

(10) Obot, N.T., Esen, E.B., Snell, K.H., Rabas, T.J., 1992, " *Pressure drop and heat transfer characteristics for air flow through spirally fluted tubes*", Int. Comm. Heat Mass Transfer, Vol. 19, pp 41-50.

(11) Obot, N.T. and Esen, E.B., 1992, "*Heat transfer and pressure drop for air flow through enhanced passages*", FHMT Report Number 007.

(12) Obot, N.T. and Esen, E.B., 1992, "*Smooth tube friction and heat transfer in laminar and transition flow*", Int. Comm. Heat Mass Transfer, Vol. 19, pp 299-310.

(13) Panchal, C.B. and France, D.M., 1983, *"Heat transfer and pressure drop in large pitch spirally indented tubes*", Int. J. Heat & Mass Transfer, Vol. 36, No. 3, pp 565-576.

(14) Ravigururajan, T.S. and Bergles, A.E., 995, "*Prandtl number influence on heat transfer enhancement in turbulent flow of water at low temperature*", Trans. Of the ASME, Vol. 117, pp 276-281.

(15) Shah, R.K. and London, A.L., 1978, "*Laminar flow forced convection in ducts*", Advances in Heat Transfer, Supplement 1, Academic Press, pp 380-384.

(16) Saha, S.K. and Chakraborty, D., 1989, "*Heat transfer and pressure drop characteristics of laminar flow in circular tube fitted with regularly spaced twisted tape elements*", Experimental Thermal and Fluid Science, Vol. 2, pp 310-322.

(17) Tariq, A., 1999. "*Augmentation heat transfer using an internally threaded tube*", M.Tech Thesis, Dept. of Mech. Engg. I.I.T. Kanpur.

(18) Tseng, C.C. and Fu, W.S., 1994, "*Enhancement of heat transfer for a tube with an inner tube insertion*", Int. J. Heat & Mass Transfer, Vol. 37, No.3, pp 499-509.